Unlimited in vitro expansion of adult bi-potent pancreas progenitors through the Lgr/R-spondin axis

Huch, Merixtell; Bonfanti, Paola; Boj, Sylvia; Sato, Toshiro; Loomans, Cindy; van de Wetering, Marc; Sojoodi, Mozhdeh; Li, Vivian; Schuijers, Jurian; Gracanin, Ana; Ringnalda, Femke; Begthel, Harry; Hamer, Karien; Mulder, Joyce; Van Es, Johan; De Koning, Eelco; Vries, Robert; Heimberg, Henry; Clevers, Hans

Published in:
EMBO Journal

Publication date:
2013

License:
Unspecified

Document Version:
Accepted author manuscript

Unlimited *in vitro* expansion of adult bi-potent pancreas progenitors through the Lgr5/Rspondin axis

Meritxell Huch[1*], Paola Bonfanti[2*], Sylvia F. Boj[1*], Toshiro Sato[1#*], Cindy J. M. Loomans[1,3], Marc van de Wetering[1], Mozhdeh Sojoodi[2], Vivian S.W. Li[1], Jurian Schuijers[1], Ana Gracanin[1], Femke Rignalda[1,3], Harry Begthel[1], Johan H. van Es[1], Eelco de Koning[1,3], Robert G.J. Vries[1], Harry Heimberg[2] and Hans Clevers[1,4]

[1] Hubrecht Institute for Developmental Biology and Stem Cell Research, Uppsalalaan 8, 3584CT Utrecht & University Medical Centre Utrecht, Netherlands

[2] Diabetes Research Center, Vrije Universiteit Brussel, Laarbeeklaan 103, B1090 Brussels, Belgium

[3] Departement of Nephrology. Leiden University Medical Center, Albinusdreef 2, 2333 ZA Leiden.

[4] Corresponding author

Current address: Department of Gastroenterology, School of Medicine, Keio University, 35 Shinanomachi, Shinnjukuku, Tokyo, 160-8582, Japan

*Equal contribution.

Corresponding author:

Hans Clevers: h.clevers@hubrecht.eu

Running title: *In vitro* expansion of pancreas progenitors

Abstract

Lgr5 marks adult stem cells in multiple adult organs and is a receptor for the Wnt-agonistic R-spondins (RSPOs). Intestinal, stomach and liver *Lgr5*$^{+}$ stem cells grow in 3D cultures to form ever-expanding organoids, which resemble the tissues of origin. Wnt signaling is inactive and *Lgr5* is not expressed under physiological conditions in the adult pancreas. However, we now report that the Wnt pathway is robustly activated upon injury by Partial Duct Ligation (PDL), concomitant with the appearance of *Lgr5* expression in regenerating pancreatic ducts. *In vitro*, duct fragments from mouse pancreas initiate *Lgr5* expression in RSPO1-based cultures, and develop into budding cyst-like structures (organoids) which expand 5-fold weekly for >40 weeks. Single isolated duct cells can also be cultured into pancreatic organoids, containing *Lgr5* stem/progenitor cells that can be clonally expanded. Clonal pancreas organoids can be induced to differentiate into duct as well as endocrine cells upon transplantation, thus proving their bi-potentiality.

Keywords: beta-cell / duct-cell / Wnt / pancreas / stem cell

Introduction

As first demonstrated for intestinal crypts (Korinek et al, 1998), Wnt signaling plays a crucial role in the regulation of multiple types of adult stem cells and progenitors (Clevers et al, 2012). The Wnt target gene *Lgr5* marks actively dividing stem cells in Wnt-driven, continuously self-renewing tissues such as small intestine and colon (Barker et al. 2007), stomach (Barker et al. 2010) and hair follicles (Jaks et al. 2008). However, expression of *Lgr5* is not observed in endodermal organs with a low rate of spontaneous self-renewal, such as liver or pancreas. In the liver, we have recently described that Wnt signaling is highly activated during the regenerative response following liver damage. *Lgr5* marks an injury-induced population of liver progenitor cells capable of regenerating the tissue after injury (Huch et al, 2013).

In the adult pancreas, Wnt signaling is inactive (Pasca di Magliano et al, 2007), yet it is essential for its development during embryogenesis (Heiser et al, 2006; Murtaugh et al, 2005). The embryonic pancreas harbors multipotent progenitor cells that can give rise to all pancreatic lineages (acinar, duct and endocrine) (Zaret et al, 2008). Injury to the pancreas can reactivate the formation of new pancreatic islets, called islet neogenesis, by mechanisms still not entirely understood but that resemble development of the embryonic pancreas (Bouwens et al, 1998; Gu et al, 2003). Lineage tracing studies have demonstrated that these "de novo beta cells" can be derived from pre-existing beta cells (Dor et al, 2004), or by conversion of alpha cells, after almost 90% beta-cell ablation (Thorel et al, 2010). Also, severe damage to the pancreas, by means of partial duct ligation or acinar ablation, can stimulate non-endocrine precursors, such as duct cells, to proliferate and differentiate towards acinar (Criscimanna et al, 2011; Furuyama et al, 2011), duct (Criscimanna et al, 2011; Furuyama et al, 2011; Kopp et al, 2011) and also endocrine lineages (including beta cells) (Xu et al, 2008; Criscimanna et al, 2011; Pan et al, 2013), suggesting the existence of a pancreas progenitor pool within the ductal tree of the adult pancreas.

The development of a primary culture system based on adult, non-transformed progenitor pancreas cells would represent an essential step in the study of the relationships between pancreas progenitor cells, their descendants and the signals required to instruct them into a particular lineage fate. Also, the production of an unlimited supply of adult pancreas cells would facilitate the development of efficient cell replacement therapies. Most of the available pancreas adult stem cell-based culture protocols yield cell populations that undergo senescence over time unless the cells become transformed. It is fair to say that no robust, long-term culture system exists today that is capable of maintaining potent, clonal expansion of adult non-transformed pancreas progenitors over long periods of time under defined conditions. Recently, endoderm progenitors derived from Embryonic Stem Cells (Sneddon et al, 2012; Cheng et al, 2012) or induced Pluriportent Stem Cells (iPS) (Cheng et al, 2012) were serially expanded, in co-culture with pancreas mesenchyme or MEFs, respectively, and gave rise to glucose-responsive beta-cells *in vitro* (Cheng et al, 2012) and glucose-sensing and insulin-secreting cells, when transplanted, *in vivo* (Sneddon et al, 2012).

We have recently described a 3D culture system that allows long-term expansion of adult small intestine, stomach and liver cells without the need of a mesenchymal niche, while preserving the characteristics of the original adult epithelium (Sato et al, 2009; Barker et al, 2010; Huch et al, 2013). A crucial component of this culture medium is the Wnt agonist RSPO1 (Kim et al, 2005; Blaydon et al, 2006), the recently reported ligand of *Lgr5* and its homologs (Carmon et al, 2011; de Lau et al, 2011). Here, we describe that Wnt signaling and *Lgr5* are strongly upregulated in remodeling duct-like structures upon injury by PDL. We exploit the Wnt-Lgr5-Rspo signaling axis to generate culture conditions that allow long-term expansion of adult pancreatic duct cells, which maintain the ability to differentiate towards both duct and endocrine lineages when provided the proper signals.

Results

Wnt signaling and *Lgr5* expression are up-regulated during pancreas regeneration following partial duct ligation (PDL)

We first sought to document Wnt pathway activation in normal adult pancreas and following acute damage. We used the *Axin2-LacZ* allele as general reporter for Wnt signaling (Leung et al, 2002; Lustig et al, 2002; Yu et al, 2005). In the head of a pancreas injured by PDL, where there is still healthy tissue, the reporter was inactive (Figure 1A), in agreement with the previous observations made with the TOPGAL Wnt reporter mice (DasGupta et al, 1999; Pasca di Magliano et al, 2007). However, after controlled injury by PDL (Watanabe et al, 1995; Xu et al, 2008), the *Axin2-LacZ* reporter was highly activated along the ductal tree of the ligated part of the pancreas (Figure 1B). *Axin2* activation in the pancreas was already detectable at day 3 post-injury, as assessed by qPCR (Figure 1C). Co-labeling with duct (pan-cytokeratin, CK) and endocrine (insulin, INS) markers revealed that the *Axin2* upregulation was restricted to the duct compartment (Figure 1D). Thus, pancreas injury by PDL led to activation of Wnt target genes in the proliferative duct cell compartment (Scoggins et al, 2000) during the regenerative response.

We have recently described that the Wnt target *Lgr5* not only marks stem cells during physiological self-renewal (e.g. in the gut), but also marks a population of liver stem cells in bile ducts that is activated after liver damage (Huch et al, 2013). We utilized the *Lgr5-LacZ* knock-in allele (Barker, et al, 2007) to determine the expression of the Wnt target *Lgr5* in the pancreas. *Lgr5* is essentially undetectable in the head of a pancreas injured by PDL (non-ligated pancreas) in agreement with the absence of Wnt signaling in the tissue under homeostatic conditions (Figure 1E). However, in the tail of the pancreas upon PDL, we observed significant *Lgr5-LacZ* reporter activity in the duct cells of the ligated pancreas, starting at day 3 and peaking at day 7 after PDL (Figure 1F and Figure 1C). No background staining was detected in wild-type mice following pancreas injury (Supplementary Figure 1A). The appearance of *de novo* expression of *Lgr5* following pancreas regeneration by PDL suggested that pancreatic *Lgr5* expression may herald *de novo* activation of regenerative stem /progenitor cells by Wnt upon injury.

Pancreatic ducts self renew *in vitro*

Given the induction of Wnt and *Lgr5* after injury, and the existence of pancreas progenitors in the ductal tree (Criscimanna et al, 2011; Furuyama et al, 2011), we reasoned that adult pancreas progenitors could be expanded from the duct cell compartment under our previously defined gut and stomach organoid culture conditions (Sato et al, 2009; Barker et al, 2010). Cultures of heterogeneous populations of pancreas cells have been previously established and typically include factors such as EGF, HGF and Nicotinamide (Bonner-Weir et al, 2000; Cardinale et al, 2011; Deutsch et al, 2001; Ramiya et al, 2000; Rovira et al, 2010; Seaberg et al, 2004; Smukler et al, 2011). Most of these

approaches yield cell populations that undergo senescence over time unless the cells are transformed.

To establish pancreas cultures, isolated pancreatic duct fragments from adult healthy mice (Figure 2A) were embedded in Matrigel containing the 'generic' organoid culture factors EGF, RSPO1 and Noggin (Sato et al 2009) to which FGF10 (Bhushan et al, 2001) and Nicotinamide were added. Under these conditions, small duct fragments formed closed structures within 24-48 hours that expanded into budding cyst-like organoids (Figure 2B). The efficiency of cyst formation from isolated ducts and subsequent organoid formation was nearly 100%. Without EGF, RSPO1 or FGF10, the cultures deteriorated after 2-5 weeks (Supplementary Figure 2A). Noggin and Nicotinamide proved to be essential to maintain the cultures >2 months (~Passage 8). The cultures maintained exponential growth with cell doubling times essentially unchanged during the culturing period (Figure 2C). Using these culture conditions, we have been able to expand the cultures by passaging at a 1:4-1:5 ratio weekly for over 10 months (Figure 2B, latest time point 9 months). These culture conditions allowed the recovery of the cells after freeze-thawing. Of note, when transplanted into imunocompromised mice, the cultures did give rise only to ductal structures, and no tumor formation was detected in any of the mice analysed (n=5), confirming the non-transformed origin of the cultured cells (Supplementary Figure 2C-D). Also, the karyotype analysis revealed that chromosome numbers were essentially normal, even after >5 months in culture (Supplementary Figure 2B).

Organoids generated from *Axin2-LacZ* and *Lgr5-LacZ* knock-in mice allowed localization of the *Axin2*- and *Lgr5*-positive cells. We observed XGAL staining in *Axin2-LacZ* pancreas organoids throughout the cysts, whereas XGAL staining in the *Lgr5-LacZ* derived pancreas organoids was mainly restricted to small budding structures (Figure 2D). These results resembled the *in vivo* situation after pancreas injury by PDL, where only the ductal buds were $Lgr5^{+}$, whereas the *Axin2* reporter showed a broader expression pattern (compare Figure1B *vs.* Figure 1F).

Prospectively isolated single pancreatic duct cells but not endocrine or acinar cells self-renew long-term *in vitro*

We then prospectively isolated the different pancreatic epithelial cells (duct, acinar and endocrine lineages) and cultured the different populations in our defined 3D culture system. A prospective isolation procedure that allows isolation of single cells of the different pancreatic epithelial cell types and maintenance of their viability in culture has not been established yet. The epithelial cell surface marker EpCAM and the high concentration of Zn^{2+} in secretory granules of endocrine cells, that allows binding of the fluorescent chelator TSQ (6-methoxy-8-p-toluenesulfonamido-quilone), were used as a basis for cell isolation. Pancreas tissue from both, WT or transgenic mice that constitutively and ubiquitously express eGFP (Okabe et al, 1997) was dissociated to single cells. After depletion of non-epithelial ($EpCAM^{-}$) and hematopoietic cells ($CD45^{+}$, $CD31^{+}$), the cell suspension was FACS-sorted in order to separate the granulated endocrine fraction ($EpCAM^{+}TSQ^{+}$) from the non-endocrine component ($EpCAM^{+}TSQ^{-}$) with high purity (>99.6%) (Figure 3A-D and Supplementary Figure 3A-

B). To rule out the possibility that endocrine cells might de-granulate during the isolation procedure and thus contaminate the non-endocrine fraction, we repeated the protocol on pancreas cells obtained from mouse insulin promoter (Mip)-RFP mice and found no RFP^+ cells in the non-endocrine fraction (Supplementary Figure 4A). The separated fractions were then tested for their ability to survive, proliferate and give rise to organoids under the above-defined conditions. Only the $EpCAM^+TSQ^-$ exocrine cells were able to generate duct-like structures that gave rise to larger organoids (1-1.5 % organoid formation efficiency) and had to be split once a week (Figure 3E). As expected, the growth pattern of the single sorted cells followed an exponential curve (Supplementary Figure 3D). The duct-derived cell cultures were maintained for more than 5 months (Figure 3E). The $EpCAM^+TSQ^+$ endocrine cells did not proliferate, but survived for at least 30 days in culture (Figure 3F).

Acino-ductal metaplasia can happen under conditions of stress or following injury (Means et al 2005; Blaine et al, 2010). To confirm that duct rather than acinar cells are the long-term expanded cells isolated from the $EpCAM^+TSQ^-$ fraction, we traced the progeny of isolated duct ($Sox9^+$) or acinar ($Ptf1a^+$) cells *in vitro*. Transgenic mice with a $Ptf1a^{CreER}$ allele, that is exclusively expressed in the acinar compartment (Kopp et al, 2012; Pan et al, 2013), or mice carrying the $Sox9^{CreER}$ allele, that is expressed predominantly (but is not absolutely restricted to) the duct cell compartment (Furuyama, et al, 2011; Kopp et al, 2012) were crossed with $Rosa26R^{YFP}$ mice and subcutaneously injected with tamoxifen as described in Supplementary Figure 5A. After the wash out period, the pancreas was dissociated and single $Sox9^{YFP+}$ or $Ptf1a^{YFP+}$ cells were FACS sorted and cultured in our defined pancreas culture medium (Supplementary Figure 5B-C). Only $Sox9^{YFP+}$ cells grew into budding organoids that expanded long term in culture, even when starting from a single cell (Supplementary Figure 5D, top panel). By contrast, the cultures derived from $Ptf1a^{YFP+}$ cells gave rise to smaller duct-like structures that were able to proliferate only for 3-4 passages, after which they arrested proliferation (Supplementary Figure 5D, bottom panel). In conclusion, these data indicated that the long-term expanding pancreas organoid cultures derive from duct cells. In conclusion, these data indicated that the long-term expanding pancreas organoid cultures derive from duct cells.

Lgr5 cells sustain the growth of pancreas organoids that have a duct cell phenotype

To test if the *Lgr5*-expressing cells maintained the growth potential of the pancreas organoids, we sorted single *Lgr5-LacZ*$^+$ cells from *in vitro* expanded organoids derived from *Lgr5-LacZ* knock-in mice (Barker et al 2007). Indeed, the isolated $Lgr5^+$ cells grew and formed organoids (Figure 4A-E) that were subsequently expanded for >4 months in culture by splitting the cultures weekly at a 1:6-1:8 ratio. The colony formation efficiency was ~16%, similar to the colony formation of Lgr5 cells of small intestine and stomach (Barker et al, 2010; Sato et al, 2011) (Figure 4C). Of note, 1.6% of the $Lgr5^{-neg}$ sorted population also grew into organoids (Figure 4C and Supplementary Figure 6). These $Lgr5^{-neg}$ derived clones rapidly re-expressed *Lgr5* (Supplementary Figure 6C-D) and expanded at a

similar ratio as their *Lgr5*$^{+}$ counterparts (Supplementary Figure 6E). This result mirrors the efficiency of colony formation of the FACS-sorted EpCAM^{+}TSQ^{-} exocrine cells from healthy tissue (1.65%, *Lgr5*^{neg} vs 1-1.5%, exocrine cells). Overall, these results demonstrated that pancreas-derived *Lgr5*$^{+}$ cells are capable of self-renewal and expansion *in vitro,* indicating that stem/progenitor cells can be activated both in organ-like structures and in secondary, single cell-derived organoids.

Organoids derived from single, FACS-sorted, *Sox9*$^{+}$ duct cells or from single isolated *Lgr5*$^{+}$ cells (FACS sorted from *Lgr5-LacZ* secondary cultures) allowed us to assess their lineage potential *in vitro*. Histologically, pancreas organoids displayed a duct-like phenotype characterized by a single-layered epithelium of cytokeratin-positive (CK) and MIC1-1C3-positive (Dorrell et al 2008) cells (Figure 5A). *Lgr5*$^{+}$ cells were readily detected in all organoids analyzed (Figure 4E), similarly as what we had observed in the cultures derived from (non-clonal) duct fragments (Figure 2D). Ki67 and Edu stainings demonstrated that only a subset of cells within the organoids proliferate (Figure 5A).

Then, we performed comparative gene expression profiling of 1-2 month old cultures and compared it to the gene expression profile of adult duct, acinar and islet cells. The overall gene expression profile of the organoid cultures clustered with the duct cell arrays, whereas it did not cluster with the gene profiles of acinar or endocrine cells (Figure 5B). Of note, among the genes whose expression pattern did cluster between the duct pancreatic cells and the organoids we found *Sox9, Krt7, Krt19* and *Spp1* (full list is provided in Supplementary Dataset S1). Comparison of the gene expression profile of the pancreas organoids and the pancreatic tissue (by *in silico* substraction), confirmed the segregation of the non-ductal pancreatic markers (like *Sst*, *Ins2*, *Gcg* and *Amy*) and the ductal markers (like *Krt7*, *Tcf2* and *Sox9*) (Figure 5C, Supplementary Dataset S2). Of note, the Wnt target genes *Lgr5*, *Ccnd1* and *Axin2* were also specifically highly expressed in the organoids (Figure 5C, Supplementary Dataset S2). As expected, Gene Set Enrichment analysis (GSEA) confirmed that the organoid cultures are enriched in genes specifically expressed in adult Sox9^{+} pancreatic duct cells (Figure 5D). Interestingly, we also observed enrichment in genes previously reported in small intestinal and pancreas stem cells, i.e. *Lgr5, Prom1, Sox9 and Lrig1* (Barker et al., 2007; Snnipert Gastroentrology 2009, Furuyama et al, 2011; Wong et al., 2012) (Figure 5D), while we found no significant enrichment in genes expressed during the developing pancreas at E14.5 or E17.5 (Figure 5E), confirming the adult nature of our pancreas progenitor cultures. To confirm this expression pattern, we performed qPCR analysis in cultures at early and late passages (Figure 5F). While some genes could be detected in pancreas organoids over time (*Pdx1*, *Sox9* and *Lgr5)*, no acinar (*Amy2*) or endocrine (*Ins*) markers were observed over several passages (Figure 5F). Immunofluorescent staining confirmed that the organoids were mainly formed by cells expressing Keratin19 (KRT19), SOX9, MUCIN-1 and PDX1 (Figure 5A) while negative for the endocrine marker Synaptophysin (SYP) (Supplementary Figure 4B). Overall, these results confirmed the pancreas progenitor and duct-like nature of the pancreas organoid cultures.

Expanded organoids give rise to both pancreatic endocrine and duct cells *in vivo*

The embryonic pancreas harbors all necessary factors and appropriate environmental cues to support the differentiation of *bona fide* pancreas progenitors to mature exocrine and endocrine cells *in situ* or when the embryonic pancreas cells are transplanted under the kidney capsule of an immunodeficient mouse. Therefore, to assess whether the organoid cells are capable of differentiating towards fully mature endocrine lineages (e.g. insulin producing cells) we developed a whole-organ morphogenetic assay based on the re-aggregation of dissociated cells from embryonic pancreas on the one hand and organoids generated from adult pancreas on the other hand (Figure 6A). This type of morphogenetic assay has been successfully used to demonstrate fate potency of both skin and thymic epithelial stem cells after expansion *in vitro* (Bonfanti et al, 2010). When embryonic pancreas derived from either mouse (E13.5) or rat (E14) was isolated, dissociated, re-aggregated and then transplanted under the kidney capsule of a immune-deficient mouse, the embryonic tissue fully developed into the 3 mature pancreas lineages: duct, acinar and endocrine cells (Supplementary Figure 7A).

Therefore, we isolated $EpCAM^{+}$ $TSQ^{-}GFP^{+}$ epithelial cells from the pancreas of CAG^{eGFP} adult mice (Okabe et al, 1997) as described above and expanded for at least 6 weeks (Supplementary Figure 3A-C), dissociated them to a single cell suspension and re-aggregated with embryonic E13 or E14 WT mouse or rat pancreas, respectively. The re-aggregates were kept overnight on a membrane and, the day after, were grafted under the kidney capsule of nude mice. After 2 or 3 weeks, mice were sacrificed and grafts harvested (Figure 6A and Supplementary Figure 7B). The transplanted re-aggregates did consistently grow pancreatic structures organized in both exocrine and endocrine areas, several of which contained $eGFP^{+}$ integrated cells (Figure 6B and Supplementary Figure 7C-D). Immunohistochemical analysis of the re-aggregates revealed that $eGFP^{+}$ cells mainly contributed to duct cells (Figure 6B, F). Of note, some $eGFP^{+}$ cells, that located outside of the ducts, downregulated cytokeratin expression and contained high level of PDX1 protein, a feature of beta cells (Figure 6B). Based on their expression of synaptophysin, approximately 5% of integrated $eGFP^{+}$ cells were of endocrine nature, 50% of which were also $insulin^{+}$ (Figure 6C,F). Quantification revealed that $eGFP^{+}$ cells differentiated into duct cells at a frequency of 70% (Figure 6F and Supplementary Figure 7F). It is important to remark that these percentages roughly correspond to those found in the differentiating embryonic pancreas *in vivo*. More importantly, we obtained the same results using a different reporter mouse that expresses CFP under the control of E-Cadherin promoter ($ECad^{CFP}$) (Figure 6D,E and Supplementary Figure 8A-C and 7E). We found that INS^{+} cells derived from cultivated organoids either from CAG^{eGFP} or $ECad^{CFP}$ reporter mice were functional and expressed C-peptide (Cppt) protein (Figure 6D,E and Supplementary Figure 7E). Cells with CFP membrane localization and cytoplasmic expression of both INS and mouse specific C-peptide were readily detected throughout the grafted area, even when the organoid cells were engrafted in a rat pancreas microenvironment, where

endogenous INS^+ cells were negative for the mouse/specific anti-Cppt antibody (Figure 6D,E and Supplementary Figure8C). This last result excluded the possibility of fusion between mouse-cultivated $eGFP^+$ or CFP^+ cells and WT rat endocrine cells. The specificity of this antibody both, in the ectopic rat pancreas and in the adult rat pancreas is shown in Figure 6 D and Supplementary Figure 8B-C. Furthermore, the cultivated $eGFP^+$ cells also gave rise to other endocrine lineages, such as $Glucagon^+$ (GCG^+) and $Somatostatin^+$ (SST^+) cells (Figure 7A,B). These cells were negative for INS, demonstrating that they had fully differentiated into mono-hormonal endocrine cells (Figure 7A,B).

Then, we assessed whether a less permissive environment would also allow the adult expanded progenitor duct cells to achieve an endocrine cell fate. We directly transplanted ~2 month-old adult duct pancreas cultures derived from both, Bl6 wt mice or EcadCFP mice into the kidney capsule of immunodeficient mice. We previously primed the 2 month-old cultures to express early endocrine markers by culturing them, 15 days prior to the transplantation, in a medium previously reported to allow ESC to acquire an endocrine fate (Kroon et al, 2008; D'Amour et al, 2006), with some modifications. We included the small molecule inhibitor ILV combined with FGF10, to induce *Pdx1* expression, (Chen et al, 2009; Bhushan et al, 2001) followed by DBZ treatment, to inhibit notch signaling (Milano et al, 2004) (Supplementary Figure 9A). This medium facilitated the expression of early endocrine progenitor markers (*Ngn3* and *ChrA*) while retained the expression of the ductal marker *Sox9*, and suppressed *Lgr5* (Supplementary Figure 9B). One month after transplantation, duct-like structures formed by $Krt19^+$ cells were readily detectable throughout the graft (Supplementary Figure 9C). Also, albeit at much lower efficiency, Insulin+ and Cpeptide+ cells (Supplementary Figure 9C-E), as well as ChrA+ cells were detected (supplementary Figure 9F).

Overall, these results conclusively demonstrate that cultured organoids derived from either sorted adult duct cells (CAG^{eGFP} or $ECad^{CFP}$ mice) or from freshly isolated ducts (Bl6 wt mice) are able to acquire both duct and endocrine fates, thus demonstrating their progenitor nature and bi-potency.

Discussion

The pancreas is a glandular organ that serves two important functions: the production of the digestive enzymes and the production of the hormones responsible of glucose homeostasis. This is mirrored in the wide range of pancreas diseases that vary from pancreatic cancer to disorders related to the glucose homeostasis, such as diabetes. While pancreas cancer is the result of the accumulation of oncogenic mutations in different epithelial cell types of the pancreas, diabetes is the result of severe reduction of functional beta cell mass. The lack of primary culture systems capable of long term expansion of primary tissue *in vitro*, hampers the development of therapeutic strategies for pancreas diseases. The replacement of functional pancreatic beta cells may be envisioned as a potential definitive cure for diabetes. Unfortunately, human islet transplantation is hampered by the scarcity of donors and the need for immune suppression and also by graft failure (Lysy et al, 2012). Therefore, alternative sources for cell therapy replacement hold promise as a potential treatment for diabetes.

Embryonic stem cells (ESC) and induced pluripotent stem cells (iPS) can be differentiated towards beta cells *in vitro* (D'Amour et al, 2006; Zhang et al, 2009; Nostro et al, 2011; Cheng et al, 2012) and *in vivo* (Soria et al, 2000; Kroon et al, 2008; Sneddon et al, 2012), but the reproducibility of such procedures has been limited (Lysy et al, 2012). In addition, undifferentiated ESCs and iPSCs are prone to form teratomas upon transplantation *in vivo*, therefore any remaining undifferentiated cell must be completely removed prior to be used for transplantation. Adult pancreas progenitors able to expand long-term *in vitro* while maintaining the potency to differentiate towards a duct or endocrine fate would potentially not encounter these limitations.

We report here that damage of adult pancreas results in the up-regulation of Wnt signaling and expression of the stem cell marker *Lgr5* in the neo-formed ducts. We exploit this Wnt-driven regenerative response to define a culture medium based on Wnt activation (RSPO1) that allows the unlimited expansion of duct fragments or even single isolated cells in a defined medium without serum. Under these conditions, pancreatic duct cells up-regulate the stem cell marker *Lgr5* (receptor for RSPO1), and self-renew while maintaining their genetic stability. Importantly, when the expanded adult progenitor cells receive the appropriate differentiation signals, as for instance the signals present in a developing embryonic pancreas, they are able to integrate into both exocrine and endocrine structures that express functional markers, demonstrating that they carry the hallmarks of bi-potent progenitors.

Confirming the importance of the Wnt/Rspo signaling to facilitate the proliferation of pancreatic adult cells, Jin et al reported (while this study was under revision) that Rspo supplementation to a 3-week pancreatic culture facilitates the expansion of pancreas cells into heterogeneous cultures. The otherwise non-defined medium contains Fetal Bovine Serum and ESC-derived conditioned medium (Jin et al, 2013).

Thus, the conditions here described, based on the induction of the Wnt-Lgr5-Rspo axis, allow the unlimited *in vitro* expansion of pancreas progenitors. The unlimited expansion potential of the adult progenitor cells may open avenues for building patient-derived disease models, as well as the development of regenerative strategies based on the expansion of adult, genetically non-modified, pancreas cells. Future optimization of the differentiation conditions may allow the generation of high numbers of specialized, functional pancreatic cells, to be used for the treatment of pancreas diseases such as diabetes.

Material and Methods

Mice lines and injury models

Generation and genotyping of the *Lgr5*^{LacZ} and *ECad*^{CFP} mice is already described in (Barker et al, 2007) and (Snippert et al. 2010) respectively. *Axin2*^{LacZ} mice were obtained from EMMA (European Mouse Mutant Archive, Germany). C57BL/6-Tg(ACTB-EGFP)1Osb/J, *Sox9*^{CreER} and *Ptf1a*^{CreER} mice were previously described (Furuyama et al, 2011; Okabe et al, 1997; Pan et al, 2013) and MipRFP mice were provided by Gérard Gradwohl (IGBMC, Strasbourg, F). Wildtype Sprague–Dawley (OFA) rats and OF1 mice were obtained from Janvier. Athymic (Swiss Nu$^{-/-}$) were supplied by Charles River Breeding Laboratories. All animals were maintained in a 12 h light cycle providing food and water ad libitum.

To induce pancreas injury, 3-6 months old mice were anesthetized, with a mixture of fluanisone:fentanyl:midazolam injected intraperitoneally at a dosage of 3.3 mg/Kg, 0.105 mg/Kg and 1.25 mg/Kg respectively. Following a median incision on the abdominal wall, the pancreas was exposed and, under a dissecting microscope, the pancreatic duct was ligated as described (Xu et al, 2008).

For lineage tracing experiments, tamoxifen (Sigma, T5648) was prepared at the concentration of 10mg/ml in corn oil (Sigma, C8267). A total dose of 20 mg of tamoxifen was given subcutaneously in 5 doses of 4 mg over a 10 days period. A washout period of 14 days preceded pancreas harvesting and dissociation to single cells.

Pancreas organoid cell culture

Pancreatic ducts were isolated from the bulk of the pancreas of mice older than 8 weeks by collagenase dissociation (Collagenase type XI 0,012% (w/v), dispase 0,012% (w/v), FBS 1% in DMEM media) at 37C. Isolated ducts were mixed with Matrigel (BD Bioscience) and seeded and cultured as we described previously (Barker et al, 2010; Sato et al, 2009). After matrigel formed a gel, culture medium was added. Culture media was based on AdDMEM/F12 (Invitrogen) supplemented with B27 (Invitrogen), 1.25 mM N-Acetylcysteine (Sigma), 10 nM gastrin (Sigma) and the growth factors: 50 ng/ml EGF (Peprotech), 10% RSPO1 conditioned media (kindly provided by Calvin Kuo), 100 ng/ml Noggin (Peprotech) or 10% Noggin conditioned media (in house prepared), 100 ng/ml FGF10 (Peprotech) and 10mM Nicotinamide (Sigma). One week after seeding, organoids were removed from the Matrigel, mechanically dissociated into small fragments, and transferred to fresh Matrigel. Passage was performed in 1:4-1:8 split ratio once per week for at least 9 months.

Prospective isolation and pancreas organoid single cell (clonal) culture

For clonogenic assays, whole pancreata were harvested from adult (8-12 weeks) mice and individually digested by collagenase (0.3 mg/ml) incubation at 37°C in a shaking incubator, and then dissociated to single cells by addition of trypsin (1 mg/ml, Sigma) and DNAse (0.4 mg/ml, Sigma); cell suspension

was filtered through a 70um cell strainer. Cell pellets were incubated with anti-mouse EpCAM/APC antibody (eBiosciences) for 30' on ice. Cells were either processed directly for FACS sorting or were enriched for epithelial cells using magnetic beads (EasySep^{TM} APC Positive selection kit or Epithelial enrichment kit, STEMCELL Technologies Inc.). Cells were re-suspended in a solution containing Propidium Iodide (PI, 1mg/ml, Sigma), and *N*-(6-Methoxy-8-Quinolyl)-*p*-Toluenesulfonamide (TSQ, 1mg/ml, Molecular Probes) and sorted on a FACSAria (Becton Dickinson). Clean separation between EpCAM^{+}TSQ^{-} and EpCAM^{+}TSQ^{+} cell populations was confirmed by a second FACS analysis and immunocytochemistry. According to the mouse strain, an additional gate for eGFP or YFP signal was used for sorting cells. Pulse-width gating excluded cell doublets while dead cells were excluded by addition of PI and gating on the negative cells.

For secondary clonal cultures, established cultures were dissociated into single cells and stained with DetectaGene Green CMFDG LacZ Gene Expression Kit (Molecular Probes) according to manufacturer's instructions. Propidium iodide staining was used to label dead cells and FSC: Pulse-width gating to exclude cell doublets.

Sorted cells (EpCAM^{+}TSQ^{-}*,* EpCAM^{+}TSQ^{+} *or Lgr5-LacZ)* were embedded in Matrigel and seeded in 96 well plates at a ratio of 1 sorted *Lgr5-LacZ* cell/well. Cells were cultured in the pancreas media described above supplemented with Y-27632 (10 µM, Sigma Aldrich) for the first 4 days. Passage was performed in split ratios of 1:4-1:8 once per week for at least 6 months.

In vitro growth curves

Expansion ratios were calculated from both sorted cells and duct fragments as follows. Pancreas organoid cultures or 20x10^{3}sorted cells were grown in our defined medium for 7 days. Then, the cultures were dissociated by incubation with TrypLE (gibco) until single cells. Cell numbers were counted by trypan blue exclusion at the indicated time points. From the basic formula of the exponential curve $y(t) = y_0 \times e^{(growth\ rate \times t)}$ (y = cell numbers at final time point; y_0 = cell numbers at initial time point; t = time) we derived the growth rate. Then, the doubling time was calculated as doubling time = ln(2)/growth rate for each time window analyzed.

Karyotyping

Organoid cultures in exponential growing phase were incubated for 1-1.5 hours with 0.05 µg/ml colcemid (Gibco). Then, cultures were dissociated into single cells using TryplE express (Gibco) and processed as described elsewhere (Huch et al, 2013). Chromosomes from 100 metaphase-arrested cells were counted.

Pancreatic morphogenetic assay

Pancreatic aggregates were obtained following a previously described protocol (Bonfanti et al, 2010), modified as follows. E13 mouse embryos (OF1) or E14 rat embryos (SD) were harvested from the

uteri under sterile conditions, transferred in 100mm Petri dishes containing HBSS supplemented with 10% FCS and stored on ice. Pancreatic tissue was removed from the embryonic abdomen and transferred into a solution containing collagenase (1mg/ml) and DNAase (0.4mg/ml) for about 5 minutes. A known number (from $75x10^3$ to 10^5) of GFP-labeled single cells dissociated from *in vitro* expanded adult organoids were mixed with an approximately 10-fold excess of unlabelled embryonic pancreatic cells. Aggregates were then transferred on a 0.8µm Isopore membrane filter (Millipore) and incubated at 37 °C for 24 h in RPMI medium supplemented with 10% FCS, before being grafted under the kidney capsule of nude mice as previously described (Bonfanti et al, 2010). Two – four weeks later the grafts were harvested and processed for cryosection and immunohistochemistry.

Pancreas organoid differentiation and kidney capsule transplantation

Pancreas organoids derived from Bl6 isolated ducts or $eGFP^+$ or $EcadCFP^+$ sorted cells were expanded *in vitro* for at least 2 months in our defined culture medium (EM) as described above. Then, the organoids were transferred into a differentiation medium (DM) to enhance their endocrine fate. To define the differentiation medium we adapted the protocols already described by d' Amour et al. (Chen et al, 2009; D'Amour et al, 2006) as follows: organoids grown in matrigel, in our defined expansion medium (EM), were removed from the matrigel by using BD cell dissociation and recovery reagent, following manufacture's instructions, and transferred to suspension plates. The cells were maintained for 3 days in RPMI medium supplemented with 0.2%FBS and 100ng/ml Activin A (Tocris BioScience). Then, the medium was changed to RPMI supplemented with 300nM ILV (indolactam-V) (Tocris BioScience), 100ng/ml Fgf10 (Peprotech) and 2%FBS for 4-5 days. After, the medium was replaced by DMEM supplemented with B27, Noggin (50ng/ml), Retinoic Acid (2uM) and KAAD-cyclopamine (0.25uM) for the following 6 days. Finally, for the last 2-4 days prior to transplantation, the medium was changed to DMEM supplemented with B27 and 10µM DBZ (Tocris BioScience). During all the differentiation protocol the cells were kept in suspension plates. After the last 2-4 days in DBZ supplemented medium, the organoids were collected and transplanted directly into the kidney capsule of nude mice using standard procedures. The grafts were allowed to grow for 1 month and then were harvested and processed for paraffin embedding and immunohistochemistry.

Pancreas organoids derived from Bl6 mice and cultured in our defined medium for at least 2 months were also directly transplanted into the kidney capsule of nude, SCID or NSG mice. The grafts were harvested 2 weeks and 3 months later and were processed for paraffin section and H&E staining, using standard techniques.

ß-galactosidase (LacZ) staining, immunohistochemistry and immunoflorescence

Tissues were fixed for 2 hours in ice-cold fixative (1% Formaldehyde; 0.2 % Glutaraldehyde; 0.02% NP40 in PBS0) and incubated o/n at RT with 1-2 mg/ml of X-gal (bromo-chloro-indolyl-

galactopyranoside) solution as we described in Barker *et al*. 2010 (Barker et al. 2010). The stained tissues were transferred to tissue cassettes and paraffin blocks prepared using standard methods. Tissue sections (4 μM) were prepared and counterstained with neutral red. For immunohistochemistry, tissues and organoids were fixed using formalin 4%, and stained using standard histology techniques as described (Barker et al, 2010). The antibodies and dilutions used are listed in Supplementary Table I. Stained tissues were counterstained with Mayer's Hematoxylin. Pictures were taken with a Nikon E600 camera and a Leica DFDC500 microscope. For whole mount immunofluorescent staining, organoids were processed as described in Barker *et al*. (Barker et al. 2010).

Tissue sections (4 μM) or cryosections from kidney capsule grafts were processed for immunoflorescent staining using standard procedures. For the paraffin embedded kidney capsule grafts citrate retrieval was performed. Antibodies and dilutions are listed in Supplementary Table I. Nuclei were stained with Hoechst33342 (Molecular Probes).

Microarray

For the expression analysis of pancreas cultures, total RNA was isolated from Sox9+ duct cells (isolated as described in Supplementary Figure 5), acinar and islets (prepared from whole pancreas after collagenase-disociation), whole adult pancreas and pancreas organoids cultured in our defined medium, using Qiagen RNAase kit following manufacture's instructions. From 500 ng to 1000 ng of total RNA were labelled with low RNA Input Linear Amp kit (Agilent Technologies, Palo Alto, CA). Universal mouse Reference RNA (Agilent) was differentially labeled and hybridized to the tissue or cultured samples. A 4X 44 K Agilent Whole Mouse Genome dual colour Microarray (G4122F) was used. Labeling, hybridization, and washing were performed according to Agilent guidelines. Microarray signal and background information were retrieved using Feature Extraction programme (V.9.5.3, Agilent Technologies). The hierarchical clustering analysis was performed in duct, acinar, islet and organoid arrays after in silico substraction of the pancreas gene array. A cut-off of 2-fold differentially was used for the clustering analsyis. GSEA was performed according to (Subramanian, et al, 2005). The gene lists and gene sets used for the analsyis are provided in the supplementary file Dataset 1. GEO accession number will be available soon.

RT-PCR

RNA was extracted from cell cultures or freshly isolated tissue using the RNeasy Mini RNA Extraction Kit (Qiagen) and reverse-transcribed using Moloney Murine Leukemia Virus reverse transcriptase (Promega). cDNA was amplified in a thermal cycler (GeneAmp PCR System 9700; Applied Biosystems, London, UK) as previously described (Huch et al, 2009). Primers used are listed in Supplementary Table II.

qPCR analysis

Total RNA was isolated from cells using RNeasy Mini RNA Extraction Kit (Qiagen) or from tissues by TRIzol protocol (Invitrogen). Preparation of cDNA from RNA was performed by reverse transcriptase reaction using SuperScript II Reverse Transcriptase (Invitrogen). For primer and probe sequence see Supplementary Table II. To avoid interference from contaminating genomic DNA, all primer sets were designed to span at least one intron. All targets were amplified (40 cycles) using gene-specific Taqman primers and probe sets (Applied Biosystems). Data were analyzed using the Sequence Detection Systems Software, Version 1.9.1 (Applied Biosystems).

Image analysis

Images of cultivated cells were acquired using either a Leica DMIL microscope and a DFC420C camera or a Nikon TE2000 inverted automated fluorescence microscope with motorized table and controlled by NIS elements AR software. Immunofluorescent images were acquired either using an upright Zeiss Axioplan2 fluorescence microscope with Hamamatsu C10600 ORKA-R2 camera or a confocal microscope (Leica, SP5) or a confocal microscope (Leica, SP8) or a confocal multiphoton Zeiss LSM710 NLO with TiSa laser microscope. Images were analyzed using Leica LAS AF Lite software (Leica SP5 confocal) or Smartcapture 3 (version 3.0.8). Confocal images were processed using Improvision VolocityLE and Zeiss Zen software.

Data analysis

All values are represented as mean ± standard error of the mean (S.E.M.). Man-Whitney non-parametric test was used. $p<0.05$ was considered statistically significant. In all cases data from at least 3 independent experiments was used. All calculations were performed using SPSS package.

Acknowledgements

We thank Joyce Mulder, Maaike van den Born, Stieneke van der Brink, Karien Hamer, Ann Demarre, Gunter Leuckx and Geert Stangé for technical assistance. The Hubrecht Imaging Center for imaging assistance. This work was supported by grants to MH (EU/236954), TS and SFB (EU/232814), VSWL and, JHvE (Ti Pharma/T3-106). PB (EMBO fellowship, EFSD/JDRF grant), HH (EU-HEALTH-F5-2009-241883, Dutch Diabetes Foundation 2007.16.001, NFSR G000609N10, NIH 1U01DK089571-01, IMIDIA).

Author's contributions

Experiments were conceived and designed by MH, PB, SFB, TS, HH, and HC. Experiments were performed by MH, PB, SFB and TS. *Lgr5*-sortings were performed by MvdW. AG helped with PCR experiments and karyotypes. MS and CJML and FR performed kidney transplants. HB helped with the immunofluorescence analysis of the kidney grafts. JHvE, EdK and RGJV discussed the project. MH,

SFB, PB and TS analyzed the data. JS and VSWL help with the microarray data. MH, SFB, PB, HH and HC wrote the manuscript, the other authors commented the manuscript.

Conflicts of interest

HC is inventor on a patent application related to this work.

References

Barker N, Huch M, Kujala P, van de Wetering M, Snippert HJ, van Es JH, Sato T, Stange DE, Begthel H, van den Born M, Danenberg E, van den Brink S, Korving J, Abo A, Peters PJ, Wright N, Poulsom R, Clevers H (2010) Lgr5(+ve) stem cells drive self-renewal in the stomach and build long-lived gastric units in vitro. *Cell Stem Cell* 6: 25-36

Barker N, van Es JH, Kuipers J, Kujala P, van den Born M, Cozijnsen M, Haegebarth A, Korving J, Begthel H, Peters PJ, Clevers H (2007) Identification of stem cells in small intestine and colon by marker gene Lgr5. *Nature* 449: 1003-1007

Bhushan A, Itoh N, Kato S, Thiery JP, Czernichow P, Bellusci S, Scharfmann R (2001) Fgf10 is essential for maintaining the proliferative capacity of epithelial progenitor cells during early pancreatic organogenesis. *Development* 128: 5109-5117

Blaine SA, Ray KC, Anunobi R, Gannon MA, Washington MK, Means AL (2010) Adult pancreatic acinar cells give rise to ducts but not endocrine cells in response to growth factor signaling. *Development* 137: 2289-2296

Blaydon DC, Ishii Y, O'Toole EA, Unsworth HC, Teh MT, Ruschendorf F, Sinclair C, Hopsu-Havu VK, Tidman N, Moss C, Watson R, de Berker D, Wajid M, Christiano AM, Kelsell DP (2006) The gene encoding R-spondin 4 (RSPO4), a secreted protein implicated in Wnt signaling, is mutated in inherited anonychia. *Nat Genet* 38: 1245-1247

Bonfanti P, Claudinot S, Amici AW, Farley A, Blackburn CC, Barrandon Y (2010) Microenvironmental reprogramming of thymic epithelial cells to skin multipotent stem cells. *Nature* 466: 978-982

Bonner-Weir S, Taneja M, Weir GC, Tatarkiewicz K, Song KH, Sharma A, O'Neil JJ (2000) In vitro cultivation of human islets from expanded ductal tissue. *Proceedings of the National Academy of Sciences of the United States of America* 97: 7999-8004

Bouwens L (1998) Transdifferentiation versus stem cell hypothesis for the regeneration of islet beta-cells in the pancreas. *Microscopy research and technique* 43: 332-336

Cardinale V, Wang Y, Carpino G, Cui CB, Gatto M, Rossi M, Berloco PB, Cantafora A, Wauthier E, Furth ME, Inverardi L, Dominguez-Bendala J, Ricordi C, Gerber D, Gaudio E, Alvaro D, Reid L (2011) Multipotent stem/progenitor cells in human biliary tree give rise to hepatocytes, cholangiocytes and pancreatic islets. *Hepatology*

Carmon KS, Gong X, Lin Q, Thomas A, Liu Q (2011) R-spondins function as ligands of the orphan receptors LGR4 and LGR5 to regulate Wnt/beta-catenin signaling. *Proceedings of the National Academy of Sciences of the United States of America* 108: 11452-11457

Chen S, Borowiak M, Fox JL, Maehr R, Osafune K, Davidow L, Lam K, Peng LF, Schreiber SL, Rubin LL, Melton D (2009) A small molecule that directs differentiation of human ESCs into the pancreatic lineage. *Nature chemical biology* 5: 258-265

Cheng X, Ying L, Lu L, Galvao AM, Mills JA, Lin HC, Kotton DN, Shen SS, Nostro MC, Choi JK, Weiss MJ, French DL, Gadue P (2012) Self-renewing endodermal progenitor lines generated from human pluripotent stem cells. *Cell Stem Cell* 10: 371-384

Chiang MK, Melton DA (2003) Single-cell transcript analysis of pancreas development. *Dev Cell* 4: 383-393

Clevers H, Nusse R (2012) Wnt/beta-catenin signaling and disease. *Cell* 149: 1192-1205

Criscimanna A, Speicher JA, Houshmand G, Shiota C, Prasadan K, Ji B, Logsdon CD, Gittes GK, Esni F (2011) Duct cells contribute to regeneration of endocrine and acinar cells following pancreatic damage in adult mice. *Gastroenterology* 141: 1451-1462, 1462 e1451-1456

D'Amour KA, Bang AG, Eliazer S, Kelly OG, Agulnick AD, Smart NG, Moorman MA, Kroon E, Carpenter MK, Baetge EE (2006) Production of pancreatic hormone-expressing endocrine cells from human embryonic stem cells. *Nat Biotechnol* 24: 1392-1401

DasGupta R, Fuchs E (1999) Multiple roles for activated LEF/TCF transcription complexes during hair follicle development and differentiation. *Development* 126: 4557-4568

de Lau W, Barker N, Low TY, Koo BK, Li VS, Teunissen H, Kujala P, Haegebarth A, Peters PJ, van de Wetering M, Stange DE, van Es JE, Guardavaccaro D, Schasfoort RB, Mohri Y, Nishimori K, Mohammed S, Heck AJ, Clevers H (2011) Lgr5 homologues associate with Wnt receptors and mediate R-spondin signalling. *Nature* 476: 293-297

Deutsch G, Jung J, Zheng M, Lora J, Zaret KS (2001) A bipotential precursor population for pancreas and liver within the embryonic endoderm. *Development* 128: 871-881

Dor Y, Brown J, Martinez OI, Melton DA (2004) Adult pancreatic beta-cells are formed by self-duplication rather than stem-cell differentiation. *Nature* 429: 41-46

Dorrell C, Erker L, Lanxon-Cookson KM, Abraham SL, Victoroff T, Ro S, Canaday PS, Streeter PR, Grompe M (2008) Surface markers for the murine oval cell response. *Hepatology* 48: 1282-1291

Furuyama K, Kawaguchi Y, Akiyama H, Horiguchi M, Kodama S, Kuhara T, Hosokawa S, Elbahrawy A, Soeda T, Koizumi M, Masui T, Kawaguchi M, Takaori K, Doi R, Nishi E, Kakinoki R, Deng JM, Behringer RR, Nakamura T, Uemoto S (2011) Continuous cell supply from a Sox9-expressing progenitor zone in adult liver, exocrine pancreas and intestine. *Nat Genet* 43: 34-41

Gu G, Brown JR, Melton DA (2003) Direct lineage tracing reveals the ontogeny of pancreatic cell fates during mouse embryogenesis. *Mechanisms of development* 120: 35-43

Heiser PW, Lau J, Taketo MM, Herrera PL, Hebrok M (2006) Stabilization of beta-catenin impacts pancreas growth. *Development* 133: 2023-2032

Huch M, Dorrell C, Boj SF, van Es JH, Li VS, van de Wetering M, Sato T, Hamer K, Sasaki N, Finegold MJ, Haft A, Vries RG, Grompe M, Clevers H (2013) In vitro expansion of single Lgr5(+) liver stem cells induced by Wnt-driven regeneration. *Nature*

Huch M, Gros A, Jose A, Gonzalez JR, Alemany R, Fillat C (2009) Urokinase-type plasminogen activator receptor transcriptionally controlled adenoviruses eradicate pancreatic tumors and liver metastasis in mouse models. *Neoplasia* 11: 518-528, 514 p following 528

Jaks V, Barker N, Kasper M, van Es JH, Snippert HJ, Clevers H, Toftgard R (2008) Lgr5 marks cycling, yet long-lived, hair follicle stem cells. *Nat Genet* 40: 1291-1299

Jin L, Feng T, Shih HP, Zerda R, Luo A, Hsu J, Mahdavi A, Sander M, Tirrell DA, Riggs AD, Ku HT (2013) Colony-forming cells in the adult mouse pancreas are expandable in Matrigel and form endocrine/acinar colonies in laminin hydrogel. *Proc Natl Acad Sci U S A* 110: 3907-3912.

Juhl K, Sarkar SA, Wong R, Jensen J, Hutton JC (2008) Mouse pancreatic endocrine cell transcriptome defined in the embryonic Ngn3-null mouse. *Diabetes* 57: 2755-2761

Kim KA, Kakitani M, Zhao J, Oshima T, Tang T, Binnerts M, Liu Y, Boyle B, Park E, Emtage P, Funk WD, Tomizuka K (2005) Mitogenic influence of human R-spondin1 on the intestinal epithelium. *Science* 309: 1256-1259

Kopp JL, Dubois CL, Schaffer AE, Hao E, Shih HP, Seymour PA, Ma J, Sander M (2011) Sox9+ ductal cells are multipotent progenitors throughout development but do not produce new endocrine cells in the normal or injured adult pancreas. *Development* 138: 653-665

Kopp JL, von Figura G, Mayes E, Liu FF, Dubois CL, Morris JPt, Pan FC, Akiyama H, Wright CV, Jensen K, Hebrok M, Sander M (2012) Identification of Sox9-dependent acinar-to-ductal reprogramming as the principal mechanism for initiation of pancreatic ductal adenocarcinoma. *Cancer cell* 22: 737-750

Korinek V, Barker N, Moerer P, van Donselaar E, Huls G, Peters PJ, Clevers H (1998) Depletion of epithelial stem-cell compartments in the small intestine of mice lacking Tcf-4. *Nat Genet* 19: 379-383

Kroon E, Martinson LA, Kadoya K, Bang AG, Kelly OG, Eliazer S, Young H, Richardson M, Smart NG, Cunningham J, Agulnick AD, D'Amour KA, Carpenter MK, Baetge EE (2008) Pancreatic endoderm derived from human embryonic stem cells generates glucose-responsive insulin-secreting cells in vivo. *Nat Biotechnol* 26: 443-452

Leung JY, Kolligs FT, Wu R, Zhai Y, Kuick R, Hanash S, Cho KR, Fearon ER (2002) Activation of AXIN2 expression by beta-catenin-T cell factor. A feedback repressor pathway regulating Wnt signaling. *J Biol Chem* 277: 21657-21665

Lustig B, Jerchow B, Sachs M, Weiler S, Pietsch T, Karsten U, van de Wetering M, Clevers H, Schlag PM, Birchmeier W, Behrens J (2002) Negative feedback loop of Wnt signaling through upregulation of conductin/axin2 in colorectal and liver tumors. *Mol Cell Biol* 22: 1184-1193

Lysy PA, Weir GC, Bonner-Weir S (2012) Concise review: pancreas regeneration: recent advances and perspectives. *Stem cells translational medicine* 1: 150-159

Means AL, Meszoely IM, Suzuki K, Miyamoto Y, Rustgi AK, Coffey RJ, Jr., Wright CV, Stoffers DA, Leach SD (2005) Pancreatic epithelial plasticity mediated by acinar cell transdifferentiation and generation of nestin-positive intermediates. *Development* 132: 3767-3776

Milano J, McKay J, Dagenais C, Foster-Brown L, Pognan F, Gadient R, Jacobs RT, Zacco A, Greenberg B, Ciaccio PJ (2004) Modulation of notch processing by gamma-secretase inhibitors causes intestinal goblet cell metaplasia and induction of genes known to specify gut secretory lineage differentiation. *Toxicological sciences : an official journal of the Society of Toxicology* 82: 341-358

Muñoz J, Stange DE, Schepers AG, van de Wetering M, Koo BK, Itzkovitz S, Volckmann R, Kung KS, Koster J, Radulescu S, Myant K, Versteeg R, Sansom OJ, van Es JH, Barker N, van Oudenaarden A, Mohammed S, Heck AJ, Clevers H (2012) The Lgr5 intestinal stem cell signature: robust expression of proposed quiescent '+4' cell markers. *EMBO J*. 31: 3079-3091

Murtaugh LC, Law AC, Dor Y, Melton DA (2005) Beta-catenin is essential for pancreatic acinar but not islet development. *Development* 132: 4663-4674

Nostro MC, Sarangi F, Ogawa S, Holtzinger A, Corneo B, Li X, Micallef SJ, Park IH, Basford C, Wheeler MB, Daley GQ, Elefanty AG, Stanley EG, Keller G (2011) Stage-specific signaling through TGFbeta family members and WNT regulates patterning and pancreatic specification of human pluripotent stem cells. *Development* 138: 861-871

Okabe M, Ikawa M, Kominami K, Nakanishi T, Nishimune Y (1997) 'Green mice' as a source of ubiquitous green cells. *FEBS letters* 407: 313-319

Pan FC, Bankaitis ED, Boyer D, Xu X, Van de Casteele M, Magnuson MA, Heimberg H, Wright CV (2013) Spatiotemporal patterns of multipotentiality in Ptf1a-expressing cells during pancreas organogenesis and injury-induced facultative restoration. *Development* 140: 751-764

Pasca di Magliano M, Biankin AV, Heiser PW, Cano DA, Gutierrez PJ, Deramaudt T, Segara D, Dawson AC, Kench JG, Henshall SM, Sutherland RL, Dlugosz A, Rustgi AK, Hebrok M (2007) Common activation of canonical Wnt signaling in pancreatic adenocarcinoma. *PloS one* 2: e1155

Ramiya VK, Maraist M, Arfors KE, Schatz DA, Peck AB, Cornelius JG (2000) Reversal of insulin-dependent diabetes using islets generated in vitro from pancreatic stem cells. *Nat Med* 6: 278-282

Rovira M, Scott SG, Liss AS, Jensen J, Thayer SP, Leach SD (2010) Isolation and characterization of centroacinar/terminal ductal progenitor cells in adult mouse pancreas. *Proceedings of the National Academy of Sciences of the United States of America* 107: 75-80

Sato T, van Es JH, Snippert HJ, Stange DE, Vries RG, van den Born M, Barker N, Shroyer NF, van de Wetering M, Clevers H (2011) Paneth cells constitute the niche for Lgr5 stem cells in intestinal crypts. *Nature* 469: 415-418

Sato T, Vries RG, Snippert HJ, van de Wetering M, Barker N, Stange DE, van Es JH, Abo A, Kujala P, Peters PJ, Clevers H (2009) Single Lgr5 stem cells build crypt-villus structures in vitro without a mesenchymal niche. *Nature* 459: 262-265

Scoggins CR, Meszoely IM, Wada M, Means AL, Yang L, Leach SD (2000) p53-dependent acinar cell apoptosis triggers epithelial proliferation in duct-ligated murine pancreas. *American journal of physiology Gastrointestinal and liver physiology* 279: G827-836

Seaberg RM, Smukler SR, Kieffer TJ, Enikolopov G, Asghar Z, Wheeler MB, Korbutt G, van der Kooy D (2004) Clonal identification of multipotent precursors from adult mouse pancreas that generate neural and pancreatic lineages. *Nat Biotechnol* 22: 1115-1124

Smukler SR, Arntfield ME, Razavi R, Bikopoulos G, Karpowicz P, Seaberg R, Dai F, Lee S, Ahrens R, Fraser PE, Wheeler MB, van der Kooy D (2011) The adult mouse and human pancreas contain rare multipotent stem cells that express insulin. *Cell Stem Cell* 8: 281-293

Sneddon JB, Borowiak M, Melton DA (2012) Self-renewal of embryonic-stem-cell-derived progenitors by organ-matched mesenchyme. *Nature* 491: 765-768

Snippert HJ, van Es JH, van den Born M, Begthel H, Stange DE, Barker N, Clevers H (2009) Prominin-1/CD133 marks stem cells and early progenitors in mouse small intestine. *Gastroenterology* 136: 2187-2194

Snippert HJ, van der Flier LG, Sato T, van Es JH, van den Born M, Kroon-Veenboer C, Barker N, Klein AM, van Rheenen J, Simons BD, Clevers H (2010) Intestinal crypt homeostasis results from neutral competition between symmetrically dividing Lgr5 stem cells. *Cell* 143: 134-144

Soria B, Roche E, Berna G, Leon-Quinto T, Reig JA, Martin F (2000) Insulin-secreting cells derived from embryonic stem cells normalize glycemia in streptozotocin-induced diabetic mice. *Diabetes* 49: 157-162

Subramanian A, Tamayo P, Mootha VK, Mukherjee S, Ebert BL, Gillette MA, Paulovich A, Pomeroy SL, Golub TR, Lander ES, Mesirov JP Gene set enrichment analysis: a knowledge-based approach for interpreting genome-wide expression profiles (2005) *Proc Natl Acad Sci U S A.*102: 15545-15550.

Thorel F, Nepote V, Avril I, Kohno K, Desgraz R, Chera S, Herrera PL (2010) Conversion of adult pancreatic alpha-cells to beta-cells after extreme beta-cell loss. *Nature* 464: 1149-1154

Watanabe S, Abe K, Anbo Y, Katoh H (1995) Changes in the mouse exocrine pancreas after pancreatic duct ligation: a qualitative and quantitative histological study. *Arch Histol Cytol* 58: 365-374

Wong VW, Stange DE, Page ME, Buczacki S, Wabik A, Itami S, van de Wetering M, Poulsom R, Wright NA, Trotter MW, Watt FM, Winton DJ, Clevers H, Jensen KB (2012) Lrig1 controls intestinal stem-cell homeostasis by negative regulation of ErbB signalling. *Nat Cell Biol.* 14: 401-408

Xu X, D'Hoker J, Stange G, Bonne S, De Leu N, Xiao X, Van de Casteele M, Mellitzer G, Ling Z, Pipeleers D, Bouwens L, Scharfmann R, Gradwohl G, Heimberg H (2008) Beta cells can be generated from endogenous progenitors in injured adult mouse pancreas. *Cell* 132: 197-207

Yu HM, Jerchow B, Sheu TJ, Liu B, Costantini F, Puzas JE, Birchmeier W, Hsu W (2005) The role of Axin2 in calvarial morphogenesis and craniosynostosis. *Development* 132: 1995-2005

Zaret KS, Grompe M (2008) Generation and regeneration of cells of the liver and pancreas. *Science* 322: 1490-1494

Zhang D, Jiang W, Liu M, Sui X, Yin X, Chen S, Shi Y, Deng H (2009) Highly efficient differentiation of human ES cells and iPS cells into mature pancreatic insulin-producing cells. *Cell research* 19: 429-438

Figure Legends

Figure 1 Induction of *Axin2* and *Lgr5* expression upon damage on adult pancreas

(A-B) *Axin2-LacZ* induction in newly formed pancreatic ducts upon PDL. *Axin2-LacZ* mice (n=6) underwent PDL as explained in Methods. Mice were sacrificed at the indicated time points and the non-ligated pancreatic tissue (Head-PDL) was separated from the ligated part (Tail-PDL). (**A)** Head-PDL and (**B)** Tail-PDL portion 13 days after injury. Arrows indicate XGAL specific staining exclusively detected in the pancreatic ducts of the ligated pancreas. Scale bar 200 μm (**A-B**, left panels), 50 μm (**A-B**, right panels). **(C)** qPCR analysis of *Axin2* and *Lgr5* mRNA in adult pancreas following PDL. Results are represented as mean ± SEM of at least 3 independent experiments. The *Hprt* housekeeping gene was used to normalize for differences in RNA input. Non-parametric Mann-Whitney test was used. ***p<0.0001. P, pancreas from a sham operated mice; H-PDL, Heat-PDL (non-affected area after PDL injury); T-PDL, Tail-PDL (affected area after PDL injury). **(D**) Representative image of a XGAL staining on an *Axin2-LacZ* pancreas after PDL, sections were co-stained either for Pancytokeratin (CK), a duct cell marker, and insulin (INS), an endocrine -cell marker. XGAL staining (reflecting *Axin2* expression) was detected exclusively in the pancreatic duct compartment. **(E-F)** *Lgr5-LacZ* induction in the ductal tree upon PDL. (**E**) Head PDL pancreas (n=6) do not show XGAL staining, suggesting *Lgr5* is not express in non-injured pancreas. (**F**) *Lgr5* reporter is detected in the Tail-PDL portion of treated mice (n=6). Scale bar 200 μm (**E-F**, left panels), 30 μm (**E-F**, right panels).

Figure 2 Establishment of the pancreas organoids from adult pancreatic ducts

(A) Cartoon representing the isolation method of the pancreatic ducts and the establishment of the pancreatic organoid culture. The pancreatic ducts were isolated from adult mouse pancreas after digestion, handpicked manually and embedded in matrigel. 24 hours after, the pancreatic ducts closed and started generating cystic structures. After several days in culture, the cystic structures started folding and having evaginations. **(B)** Representative serial DIC images of a pancreatic duct isolated and embedded in matrigel (day 0) and its growth at the indicated time points (top row). Representative image of a pancreas organoid culture at different time points. Magnifications: 10x (days 0, 2, 4, 6, 8), 4x (day 10 onwards). **(C)** Growth curves of pancreas organoids originated from isolated pancreatic ducts cultured in expansion conditions. Note that the cultures followed an exponential growth curve within each time window analyzed. Graphs illustrate the number of cells counted per well at each passage from passage P1-P3 (top), P5-P7 (middle) and P10-P12 (bottom). The doubling time (hours) is indicated in each graph. Data represents mean± S.E.M., n=2. (**D**) Representative DIC images of XGAL staining in WT, *Axin2-LacZ* and *Lgr5-LacZ* derived pancreas organoids.

Figure 3 Isolation and *in vitro* expansion of single, endocrine-depleted pancreatic epithelial cells

(A) Representative fluorescence-activated cell sorting (FACS) plot illustrating the distribution of

EpCAM^{+} and EpCAM^{-} cells from dissociated adult mouse pancreas, following epithelial cell enrichment by magnetic beads as described in methods. **(B)** Representative FACS plot showing the distribution of EpCAM^{+} non-granulated TSQ^{-} epithelial cells and EpCAM^{+} granulated TSQ^{+} endocrine cells. **(C)** EpCAM^{+}TSQ^{+} and EpCAM^{+}TSQ^{-} sorted fractions were cytocentrifuged and immunostained (red) for Synaptophysin (SYP), Amylase (AMY) and pancytokeratin (CK); nuclei were counterstained with Hoechst 33342 (blue). Magnification: 40x. **(D)** Representative FACS analysis of purity of sorted EpCAM^{+}TSQ^{-} cells indicating that this population is isolated with high purity (>99.6%). **(E)** EpCAM^{+}TSQ^{-} sorted single cells were assessed for their growth potential in 3D expansion culture conditions: this population gave rise to organoids that could be expanded for many passages (>5months). **(F):** EpCAM^{+}TSQ^{+} sorted single cells were assessed for their growth potential under the same conditions: endocrine TSQ^{+} cells survived in culture but did not proliferate. Scale bars: 30 m.

Figure 4 Clonal expansion of single *Lgr5* cells derived from *Lgr5-LacZ* pancreatic organoids

(**A-E**) Lgr5^{+} cells were sorted from *Lgr5-LacZ* derived pancreas organoids cultured for 20-25 days in our defined medium. Organoid formation efficiency was analysed 12 days after seeding. **(A)** Representative image of a FACS plot of wildtype (left) and *Lgr5-LacZ* (right) pancreas organoids stained with Detectagene Green CMFDG (for detecting beta-galactosidase expression) and EpCAM (for selecting epithelial cells). **(B)** Representative image of cultures derived from 500 sorted cells from the high (*Lgr5*^{hi}) or 500 sorted cells derived from the negative fraction (*Lgr5*^{neg}) 12 days after seeding. **(C)** Graph showing the % of colony formation efficiency of the *Lgr5*^{hi} and *Lgr5*^{neg} fractions. **(D)** Representative serial DIC images showing the outgrowth of pancreatic organoids originated from a single *Lgr5-LacZ*$^{+}$cell. **(E)** Representative DIC image of XGAL staining in a 12 days-old clonal culture derived from *Lgr5*^{hi} fraction.

Figure 5 Characterization of *in vitro* expanded organoids from single cells

(**A**) Pancreatic organoids cultured in expansion medium show a ductal-like phenotype. FACS sorted epithelial cells were isolated as shown in Figure 3 and 4, plated in 3D matrigel expansion conditions and cultured for 7 - 9 passages before being processed for histological analysis. Organoids were stained with anti-pancytokeratin (CK), anti-PDX1, anti-mucin 1 (MUC1), anti-SOX9, anti-cytokeratin19 (CK19) and anti-MIC1-1C3 which revealed their duct-like phenotype. Cells were proliferating, as illustrated by anti-KI67 and Edu immunostaining. Scale bars: 35 m. (**B**) Hierarchical clustering analysis of genes differentially expressed among pancreatic organoid cultures, duct, acinar and istet pancreatic lineages. Unsupervised hierarchical clustering analysis shows that the pancreas organoid arrays cluster with the ductal array while the acinar and islet profiles clustered in a separate

tree. (**C**) Heat map of two independent clonal pancreas organoid cultures performed after subtracting pancreas tissue expression levels. Representative organoid-, duct-, endocrine- and exocrine-specific genes are listed on the right. Red, upregulated; green, downregulated. (**D-E**) Gene set enrichment analysis (GSEA) revealed that pancreas organoid cultures express a significant amount of genes contained in signatures of adult duct cells and intestinal stem cells (Munoz et al, 2012) (**D**), while they were not enriched in gene sets representing embryonic pancreas at E14.5 or E17.5 (Juhl et al, 2008) (**E**). (**F**) Quantitative PCR showing relative fold changes of *Pdx1, Sox9, Lgr5, Amy* and *Ins* mRNA levels in partial duct ligated pancreas (CTRL) and cultured organoids at early (EP, passage 2-3) and late passages (LP, passage 7-9). Data represents mean ± S.E.M (n=2, independent cultures).

Figure 6 *In vitro* expanded organoids from single epithelial cells give rise to endocrine and duct cells when grafted *in vivo* in a developing pancreas

(A-F) Pancreas organoid cultures were derived from CAG^{eGFP+} mice or $ECad^{CFP+}$ mice as described in Figure 3 and supplementary Figure 3. The cultures were clonally expanded *in vitro* for 4 to 6 passages before dissociation to single cells. Dissociated $eGFP^+$ or $ECad^{CFP+}$ cells were re-aggregated with WT embryonic E13 mouse (**B-C**) or E14 rat (**D-E**) pancreas. The re-aggregates were kept on a filter membrane O/N and then grafted under the kidney capsule of nude mice. The grafts were were harvested and analyzed 2-3 weeks after. The re-aggregates consistently grew and gave rise to pancreatic tissue, as illustrated in Supplementary Figure 7A. (**A**) Schematic representation of the pancreatic morphogenetic assay. **(B)** Representative confocal microscopy image showing incorporation of $eGFP^+$ cells (green) into $pancytokeratin^+$ (CK, red) cells, located in pancreatic duct structures; these $eGFP^+$ cells also express low levels of PDX1 (blue). Other $eGFP^+$ cells (white arrow) aggregated in islet-like structures near the ducts, dowregulated CK and expressed high levels of PDX1 (blue). Scale bars: 35 m. (**C**) Confocal microscopy demonstrates that cultured $eGFP^+$ (green) cells differentiate into beta cells and express both synaptophysin (SYP, red) and insulin (INS, blue). Scale bars: 20 m. (**D**) Confocal microscopy image illustrating mouse INS^+Cppt^+ cells derived from $ECad^{CFP+}$ grafted cells. Note that the INS^+Cppt^+ cells are incorporated into an embryonic rat pancreas, where rat INS^+ cells are negative for mouse specific Cppt staining. Scale bars: 30 m. (**E**) High magnification of an $ECad^+INS^+Cppt^+$ grafted cell (panel D) that displays membrane localization of CFP and cytoplasmic staining for INS and mouse Cppt. Scale bar: 20 m. (**F**) Histogram showing the average quantification of differentiation of $eGFP^+$ cells engrafted into each re-aggregate under the kidney capsule. Endocrine (SYP^+), insulin (INS^+), duct cells (CK^+); others: cells expressing neither duct nor endocrine markers. Average number/graft ± S.E.M. n=11 grafts from 6 independent cultures.

Figure 7 *In vitro* expanded organoids give rise to Glucagon (Gcg) and Somatostatin (Sst) mono-

hormonal cells in vivo

Pancreas organoid cultures derived from sorted CAG^{eGFP+} cells and expanded for at least 2 months in culture were grafted as described in Figure 6. Two weeks after transplantation the kindey grafts were harvested and the grafted $eGFP^+$ cells were evaluated for the expression of glucagon (Gcg) and Somatostatin (Stt). (**A-B**) Representative images illustrating that $eGFP^+$ cells (green) differentiate towards Gcg^+ (**A**) or Stt^+ (**B**) cells *in vivo*. Note that both, Gcg^+ and Stt^+ cells do not express INS (insulin, blue), indicating that the organoid derived $eGFP^+$ cells have fully differentiated into mono-hormonal cells *in vivo*. Scale bars = 20 m.

Supplementary Figure 1: X-gal staining in a PDL wild type (WT) control mouse

WT littermate control mice (n=5) underwent PDL surgery. Tissues were harvested and processed for XGAL staining. Representative image of a WT pancreas stained for XGAL 14 days after PDL. No unspecific staining was observed.

Supplementary Figure 2: Pancreatic organoid cells did not show any sign of transformation in culture. (**A**) Pancreatic ducts-derived organoids were cultured as described in Methods (complete), or in the absence of individual components, as indicated. Each horizontal bar represents an independent experiment. Pancreatic organoids grow only when cultured with all the growth factors. (**B**) Genetic stability of the pancreas organoids cultured for long time. Representative image of a chromosome spread representing a normal count (n=40) of a metaphase of a cell cultured for 175 days. The table illustrates the % of cells with chromosomal counts <39, =39, =40 and >40. (**C-D**) Representative H&E staining of a organoid-derived graft transplanted under the kidney capsule and harvested 2 weeks (**C**) and 2 months (**D**) later. Only ductal-like structures surrounded by ECM (extra cellular matrix) (#) are detected at both time points. No signs of transformation were observed in the transplanted ductal cells (arrows). # indicates the ECM formed around the engrafted pancreatic organoid derived cells.

Supplementary Figure 3: Isolation and *in vitro* expansion of endocrine-depleted pancreatic epithelial cells from eGFP transgenic mice

(A) Fluorescence-activated cell sorting (FACS) plot illustrating the distribution of $eGFP^+$ live cells dissociated from an adult CAG^{eGFP+} mouse pancreas. $eGFP^+$ cells were sorted on the basis of EpCAM and TSQ expression. (**B**) $EpCAM^+TSQ^-$ cells were checked for purity (>99.9%) and plated in 3D expansion conditions. (**C**) $eGFP^+$ cells gave rise to expanding organoids as from *Lgr5LacZ* and WT mouse pancreas cells. (**D)** Growth curve of pancreas organoids originated from $EpCAM^+TSQ^-$ sorted single cells cultured in our defined medium. Graph showing the number of cells counted per well at each passage. The cultures were expanded and split approximately once a week. Data represents

mean± S.E.M., n=2.

Supplementary Figure 4: Endocrine markers are not expressed in freshly isolated EpCAM^{+}TSQ^{-} cells and in expanding organoids

(A) EpCAM^{+}TSQ^{+} and EpCAM^{+}TSQ^{-} sorted fractions from MipRFP mice were cytocentrifuged and direct RFP fluorescence detected and imaged by confocal microscope (red); nuclei were counterstained with Hoechst 33342 (blue). Scale bars = 20 m. **(B)** Immunohistochemistry demonstrating absence of endocrine marker synaptophysin in an organoid growing for 6 passages *in vitro* (SYP, green). Positive control, adult pancreas tissue (SYP, green). Nuclei are counterstained with Hoechst 33342, white. Scale bars = 20 m.

Supplementary Figure 5: Isolation and *in vitro* expansion of single, endocrine-depleted Sox9+ and Ptf1a+ pancreatic epithelial cells

(**A**) Schematic representation of Tamoxifen administration to Sox9CreERxR26$^{fl/flYFP}$ and *Ptf1a*^{CreER}*xR26*$^{fl/flYFP}$ mice. 20mg of Tamoxifen were injected subcutaneously over a period of 10 days. A wash out period of 2 weeks followed before pancreas harvesting and dissociation to single cells. (**B-C**) Fluorescence-activated cell sorting (FACS) plot illustrating the distribution of YFP^{+}EpCAM^{+}TSQ^{-} cells derived from either *Sox9*^{CreER}*xR26*$^{fl/flYFP}$ or *Ptf1a*^{CreER}*xR26*$^{fl/flYFP}$. (**D**) Schematic representation of cultures of YFP^{+} cells from *Sox9*^{CreER}*xR26*$^{fl/flYFP}$ and *Ptf1a*^{CreER}*xR26*$^{fl/flYFP}$. Images show that Sox9^{+} cells give rise to large duct-like structures that can be expanded for several weeks, while Ptf1a^{+} cells generate small duct-like structures that cannot be amplified for more than 3-4 passages. Magnification: 4x.

Supplementary Figure 6 Lgr5 negative clones re-express *Lgr5* after culturing

Pancreas organoids derived from *Lgr5-LacZ* mice were grown for at least 2 weeks in culture before being processed for b-galactosidase FACS analysis as described in figure 4. (**A**) Representative fluorescence-activated cell sorting (FACS) plot illustrating the distribution of *Lgr5*$^{+}$ cells from dissociated *Lgr5-LacZ* derived pancreas cultures stained with Detectagene Green CMFDG (to detect beta-galactosidase expression). Representative fluorescence images illustrate *Lgr5* negative (left panel) and *Lgr5* positive (right panel) cells after sorting. (**B**) *Lgr5* expression was determined on the positive and negative sorted fractions by quantitative qPCR analysis. Results are expressed as 2deltaCt. *Hprt* expression was used to normalize the results. (**C-E**) Both, positive and negative *Lgr5* sorted populations were seeded in matrigel and cultured in our defined culture medium. The colony formation efficiency of the positive (Lgr5^{+}) and negative (Lgr5^{neg}) fractions is illustrated in Figure 4 (16.03%, Lgr5^{+} vs 1.6%, Lgr5^{neg}). Lgr5 expression was determined in clones started from both Lgr5^{+} and Lgr5^{neg} fractions at 12 days (**C**) and 3 weeks (**D**) after seeding. (**C**) Representative DIC image of an Xgal stained organoid derived from a clone established from the *Lgr5* negative fraction. B-

galactosidase (blue) staining indicates that *Lgr5* expression is re-activated as early as 12 days after seeding. Magnification 4x. (**D**) Quantitative PCR showing relative fold change of *Lgr5* expression normalized by *Hprt* in organoids derived from *Lgr5* positive and negative single cell derived clones. At 3 weeks after seeding *Lgr5* clones derived from the *Lgr5* neg population re-expressed *Lgr5* at the same level as the *Lgr5*+ derived clones. Data represents mean ± S.E.M (n=2, independent cultures). (**E**) Clones started from the negative fraction were serially passaged for at least 2 months in a 1:4 split ratio. Magnification 4x.

Supplementary Figure 7: *In vivo* morphogenetic assay for the pancreas. The developing organ facilitates the incorporation and differentiation of adult cultured pancreas organoid cells.
(**A**) Pancreatic morphogenetic assay: embryonic mouse (E13) or rat (E14) pancreata are dissociated and then re-aggregated and grafted under the kidney capsule of nude mice. In the following 2 - 3 weeks time window the organ develops into all the 3 pancreatic lineages: duct cells (CK^+, red), endocrine cells (INS^+, blue) and acinar cells (AMY^+, red). Nuclei are counterstained with Hoechst (white). (**B**) Schematic representation of the morphogenetic assay where the embryonic pancreas is mixed with cultured organoid cells derived from either $CAGe^{GFP+}$ or $ECad^{CFP}$ mice. Kidney capsule grafts were harvested and further processed for cryosection and immunohistochemistry. (**C**) $eGFP^+$ cells (green) were incorporated into both, duct (right panel) and endocrine (left panel) structures. Insets show higher magnification of $eGFP^+$ endocrine cells co-expressing both insulin (INS, blue) and synaptophysin (SYP, red) endocrine markers. (**D**) $eGFP^+$ cells derived from the cultured organoids differentiated into endocrine cells co-expressing both INS (blue) and SYP (red) endocrine markers. Insets show high magnifications of $eGFP^+INS^+$ cells. Magnifications: 20x. (**E**) $EcadCFP^+$ mouse derived pancreas cultures were re-aggregated and grafted with rat embryonic pancreas (E14) as described. Representative confocal image of INS^+ (blue), mouse $Cppt^+$ (red) and $EcadCFP^+$ mouse cells. All nuclei were counterstained with Hoechst 33342 (white, **C-E**). **(F)** Histogram showing the percentage ± S.E.M of endocrine (SYP^+), duct cells (CK^+) and other cell types (others) detected by double immunofluorescence in 11 grafts from 6 independent cultures.

Supplementary Figure 8: Characterization of ECadCFP mouse pancreas and assessment of mouse specificity of anti-Cppt antibody. (A) Confocal microscopy image illustrating the membrane localization of CFP (green) in the adult mouse pancreas of $ECad^{CFP}$ mice. Note that Endocrine INS^+ (blue) and SYP^+ (red) cells are all positive for CFP. Scale bar: 35 m **(B)** INS^+ (blue) cells of the adult mouse pancreas stain positive for the mouse specific anti-Cppt while INS^+ (blue) cells of the adult rat pancreas **(C)** are negative for the mouse Cppt staining, demonstrating species-specificity of the anti-Cppt antibody. Scale bar: 35 m (**B**) and scale bar: 40 m (**C**).

Supplementary Figure 9

(A) Scheme of differentiation procedure of the pancreas organoids. The detailed differentiation protocol is described in Material and Methods. ILV, indolactam-V; FGF10, fibroblast growth factor 10. **(B)** Quantitative PCR showing relative fold changes of *Lgr5, Pdx1* and *Chra* mRNA levels in pancreas organoids cultured in our defined expansion medium (EM) or after being treated with the differentiation protocol (DM) described in (**A**). Data shows fold change comparing DM *vs.* EM levels after normalizing by *Hprt*. *Neurog3* was detected by semi-quantitative RT-PCR in 2 independent cultures of pancreas organoids differentiated with the protocol described in (**A**). *Hprt* was used as internal reference. Embryonic E14 pancreas RNA was used as + control. Representative image is shown. (**C-F**) Organoids derived from Bl6 mouse (**C-D, F**) or ECadCFP mouse (**E**) expanded for at least 2 months in culture were differentiated as described in (**A**), and transplanted directly into the kidney capsule of nude mice. One month after transplantation, the kidneys were collected and the grafts analyzed for the presence of duct and endocrine cells from the donor organoid cells. **(C)** Pancreas organoids readily generated duct-like structures, as detected by PCK (pancytokeratin) staining. Some cells delaminated from the ducts and differentiated towards endocrine, INS (insulin) positive, cells. (**D**) Representative confocal image of organoid derived cells expressing both INS and mCPPT (mouse specific C-peptide) in a 1 month-old graft. (**E**) Representative confocal image of transplanted ECad-CFP positive cells co-expressing INS and mCPPT. (**F**) KRT19 (keratin 19) duct-like structures surrounded by endocrine committed cells expressing CHRA (Chromogranin A) were detected 1 month after transplantation. Representative confocal image is shown. In all cases, Nuclei were stained with Hoechst.

Supplementary Table I: Antibody list

Supplementary Table II: Primer list

Supplementary Dataset 1: Gene lists used for the microarray analysis and GSEA

Figure 1

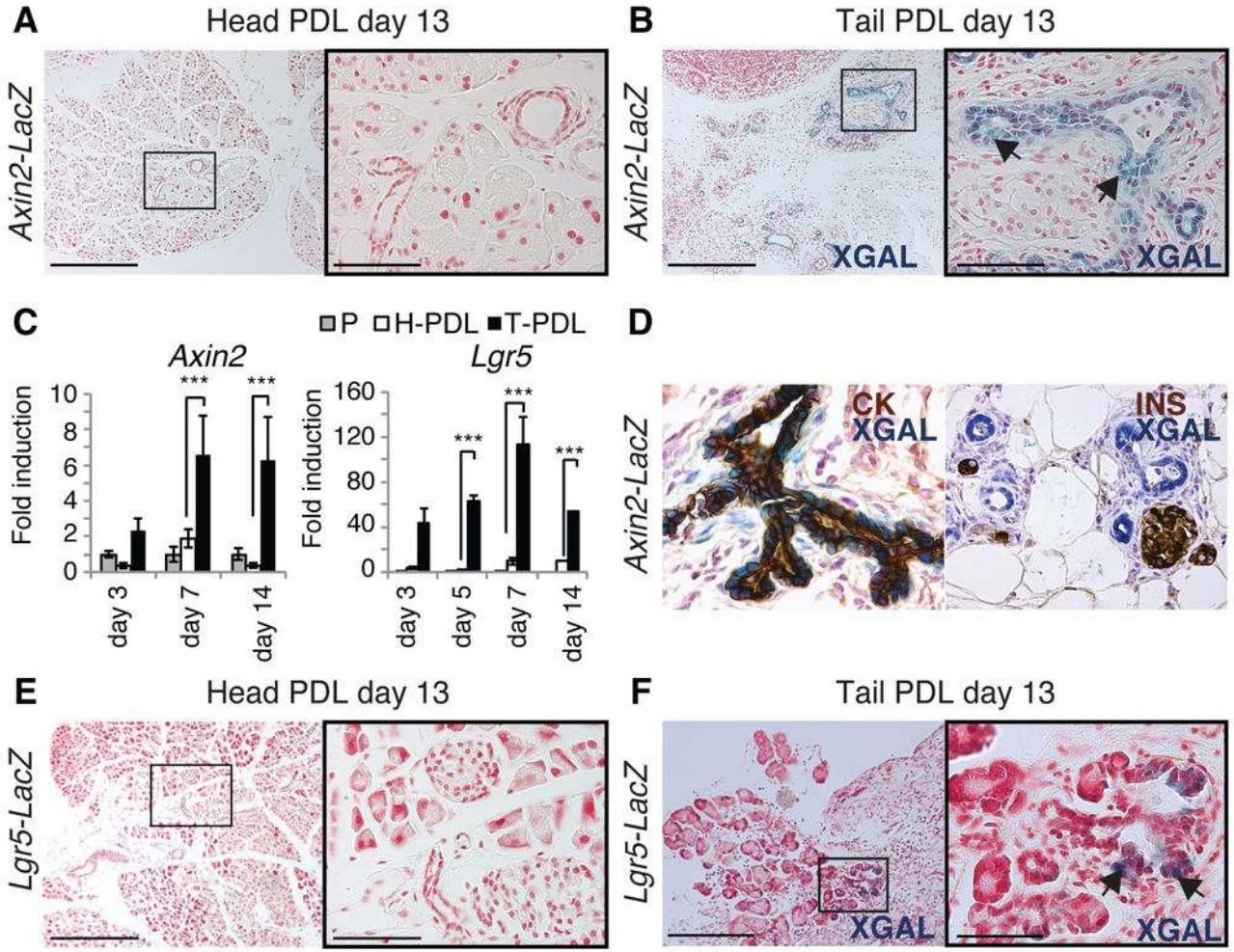
A
Head PDL day 13
Axin2-LacZ
B
Tail PDL day 13
Axin2-LacZ
XGAL
XGAL
C
P H-PDL T-PDL
Axin2
Lgr5
Fold induction
10
8
6
4
2
0
***
***
day 3
day 7
day 14
Fold induction
160
120
80
40
0
***
***
***
day 3
day 5
day 7
day 14
D
Axin2-LacZ
CK
XGAL
INS
XGAL
E
Head PDL day 13
Lgr5-LacZ
F
Tail PDL day 13
Lgr5-LacZ
XGAL
XGAL

Figure 2

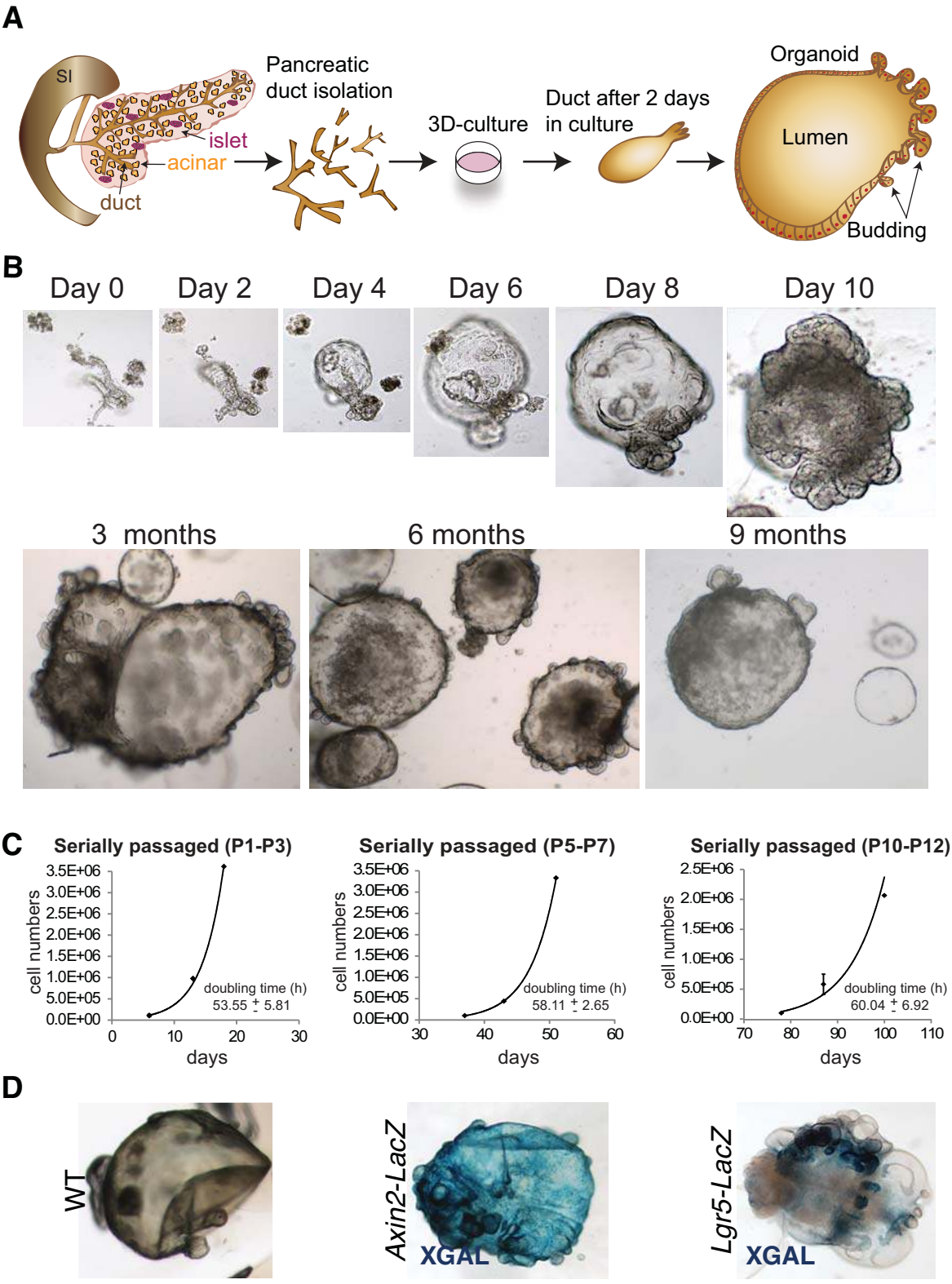
A
SI
islet
acinar
duct
Pancreatic
duct isolation
3D-culture
Duct after 2 days
in culture
Organoid
Lumen
Budding
B
Day 0
Day 2
Day 4
Day 6
Day 8
Day 10
3 months
6 months
9 months
C
Serially passaged (P1-P3)
cell numbers
3.5E+06
3.0E+06
2.5E+06
2.0E+06
1.5E+06
1.0E+06
5.0E+05
0.0E+00
0
10
20
30
days
doubling time (h)
53.55 ± 5.81
Serially passaged (P5-P7)
cell numbers
3.5E+06
3.0E+06
2.5E+06
2.0E+06
1.5E+06
1.0E+06
5.0E+05
0.0E+00
30
40
50
60
days
doubling time (h)
58.11 ± 2.65
Serially passaged (P10-P12)
cell numbers
2.5E+06
2.0E+06
1.5E+06
1.0E+06
5.0E+05
0.0E+00
70
80
90
100
110
days
doubling time (h)
60.04 ± 6.92
D
WT
Axin2-LacZ
XGAL
Lgr5-LacZ
XGAL

Figure 3

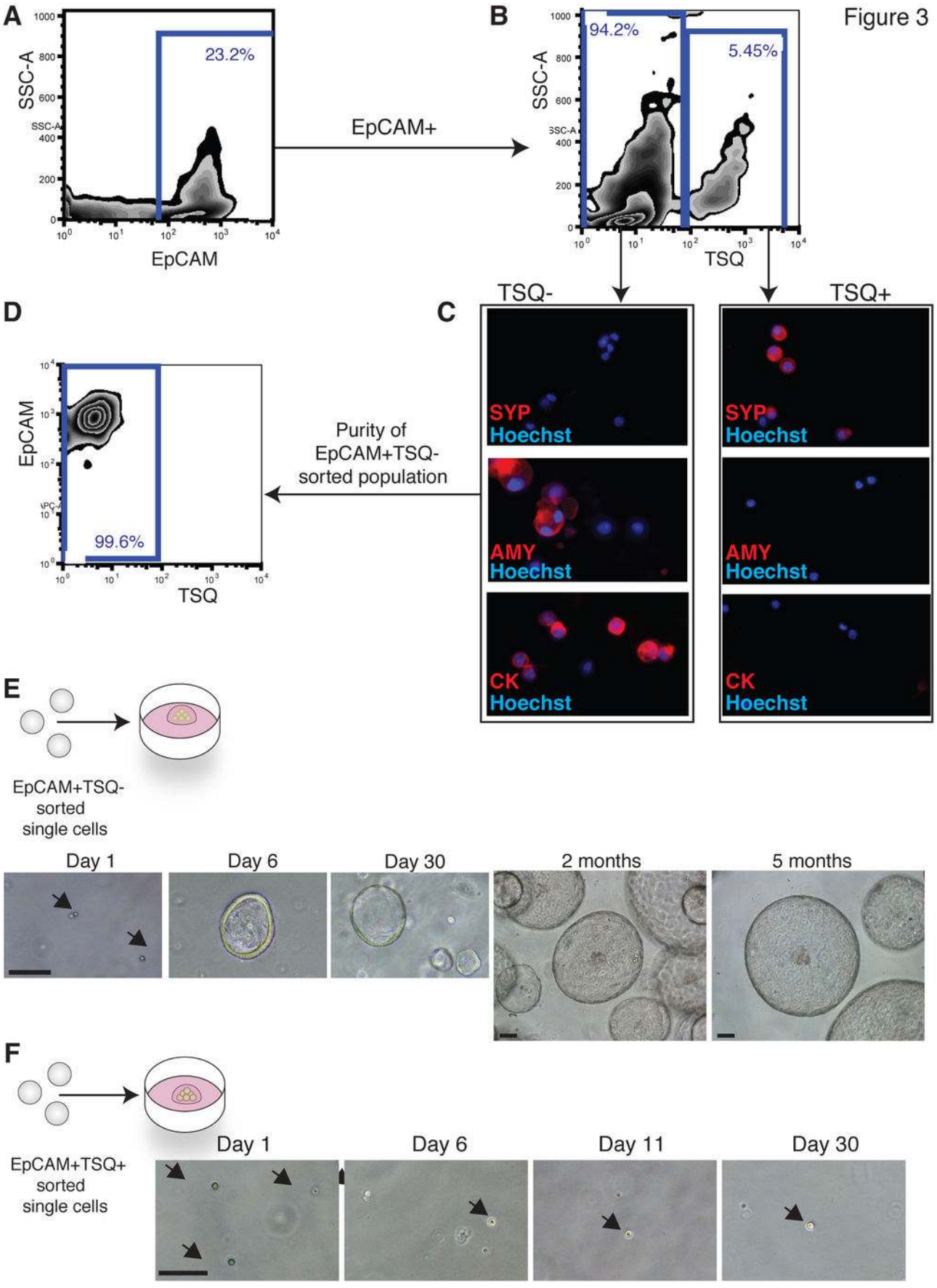
A
SSC-A
23.2%
EpCAM
EpCAM+
B
SSC-A
94.2%
5.45%
TSQ
TSQ-
TSQ+
C
SYP
Hoechst
AMY
Hoechst
CK
Hoechst
D
EpCAM
99.6%
TSQ
Purity of
EpCAM+TSQ-
sorted population
E
EpCAM+TSQ-
sorted
single cells
Day 1
Day 6
Day 30
2 months
5 months
F
EpCAM+TSQ+
sorted
single cells
Day 1
Day 6
Day 11
Day 30

Figure 4

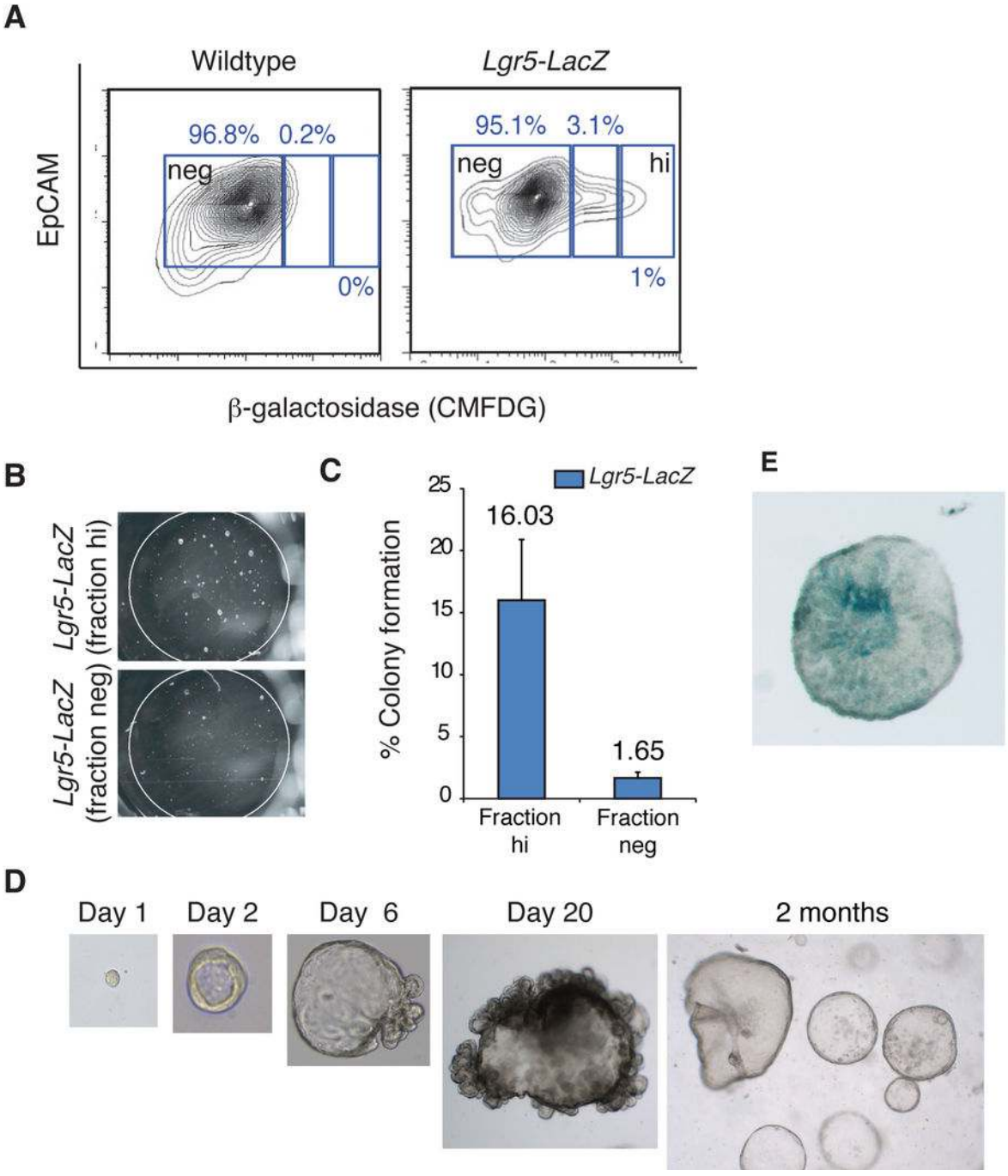
A
Wildtype
Lgr5-LacZ
EpCAM
96.8%
0.2%
neg
0%
95.1%
3.1%
neg
hi
1%
β-galactosidase (CMFDG)
B
Lgr5-LacZ (fraction hi)
Lgr5-LacZ (fraction neg)
C
Lgr5-LacZ
% Colony formation
25
20
15
10
5
0
16.03
1.65
Fraction hi
Fraction neg
E
D
Day 1
Day 2
Day 6
Day 20
2 months

Figure 5

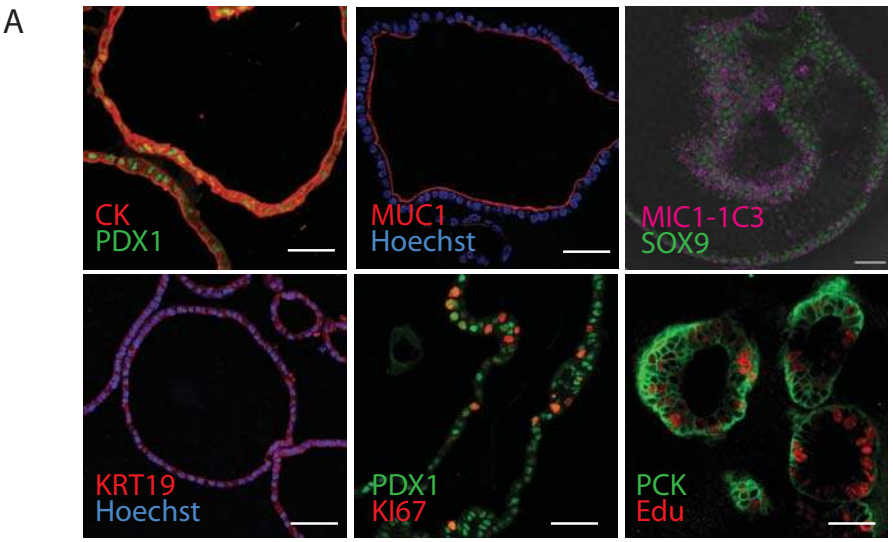
A
CK
PDX1
MUC1
Hoechst
MIC1-1C3
SOX9
KRT19
Hoechst
PDX1
KI67
PCK
Edu

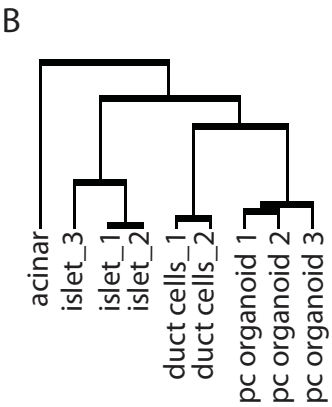
B
acinar
islet_3
islet_1
islet_2
duct cells_1
duct cells_2
pc organoid 1
pc organoid 2
pc organoid 3

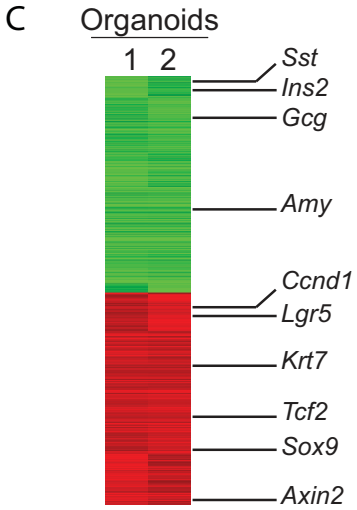
C
Organoids
1
2
Sst
Ins2
Gcg
Amy
Ccnd1
Lgr5
Krt7
Tcf2
Sox9
Axin2

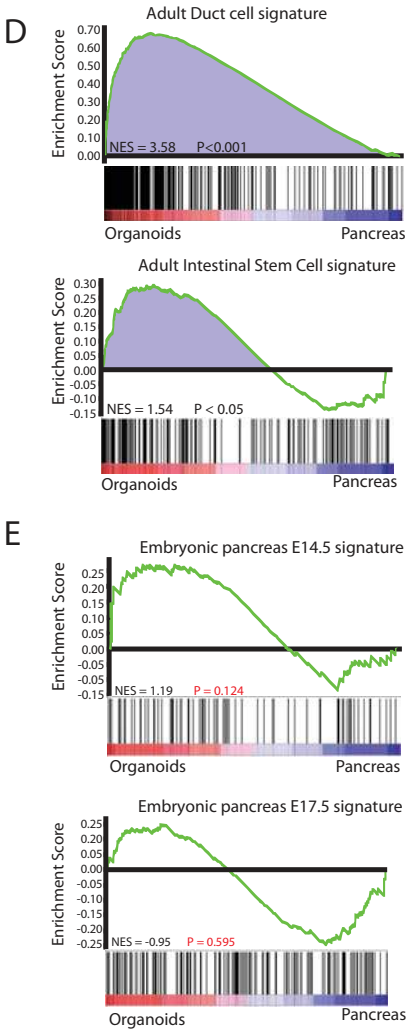
D
Adult Duct cell signature
Enrichment Score
NES = 3.58
P<0.001
Organoids
Pancreas
Adult Intestinal Stem Cell signature
NES = 1.54
P < 0.05
E
Embryonic pancreas E14.5 signature
NES = 1.19
P = 0.124
Embryonic pancreas E17.5 signature
NES = -0.95
P = 0.595

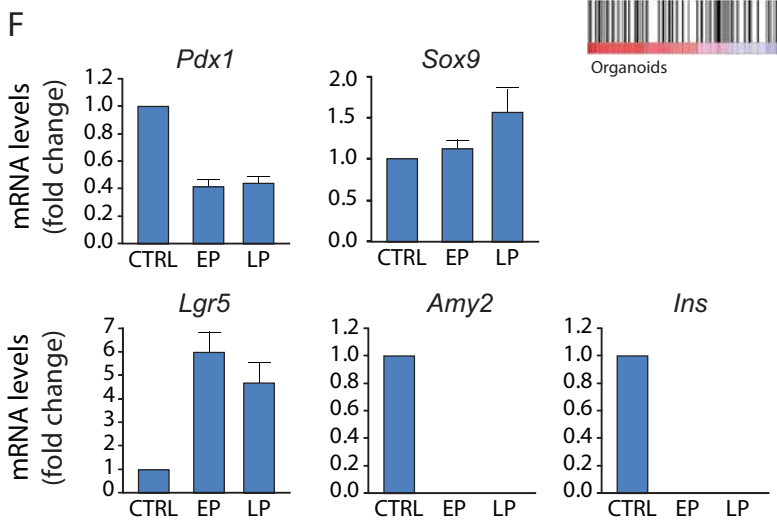
F
Pdx1
Sox9
Lgr5
Amy2
Ins
mRNA levels
(fold change)
CTRL
EP
LP

Figure 6

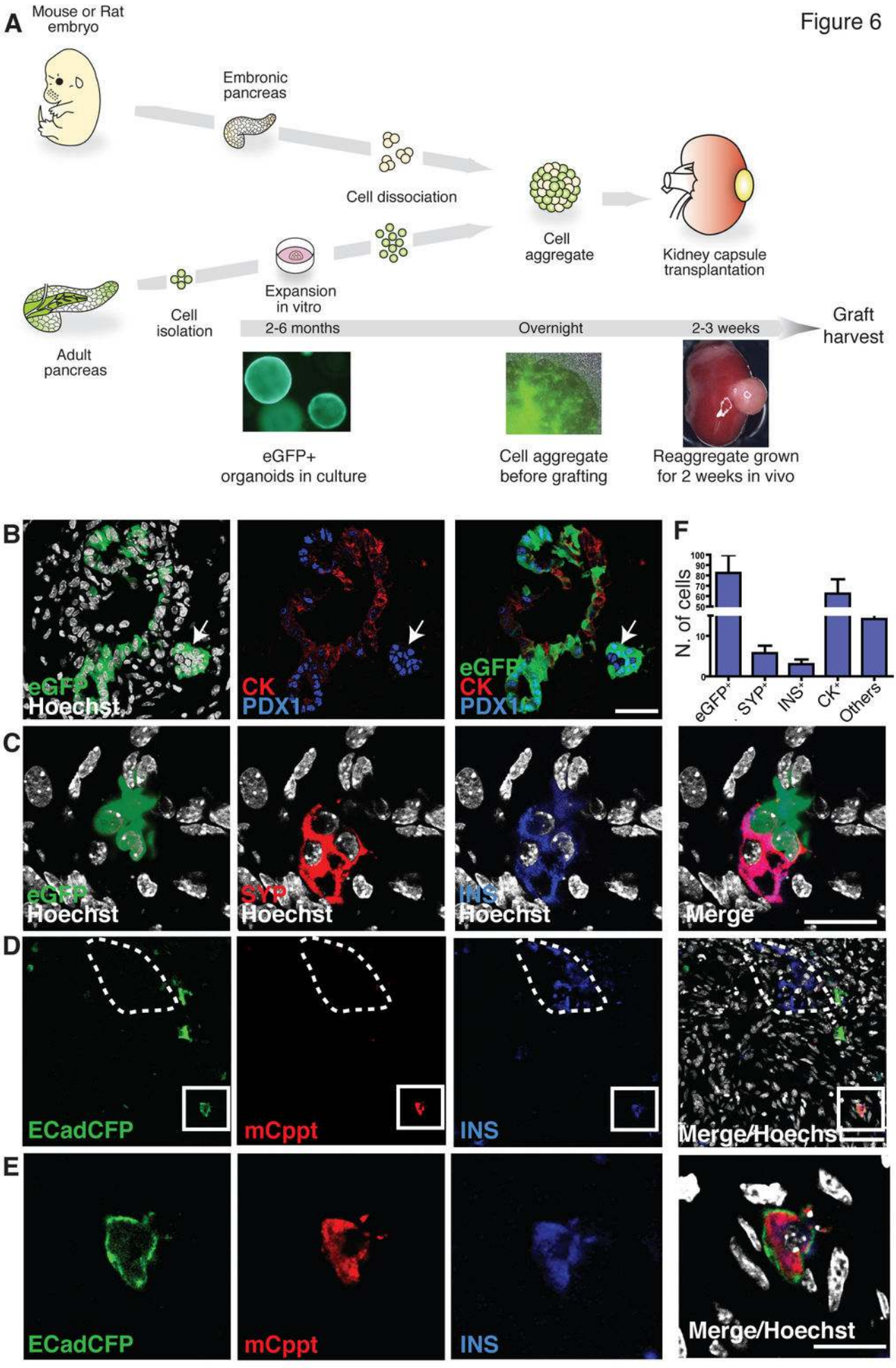
A
Mouse or Rat embryo
Embronic pancreas
Cell dissociation
Cell aggregate
Kidney capsule transplantation
Adult pancreas
Cell isolation
Expansion in vitro
2-6 months
Overnight
2-3 weeks
Graft harvest
eGFP+ organoids in culture
Cell aggregate before grafting
Reaggregate grown for 2 weeks in vivo
B
eGFP
Hoechst
CK
PDX1
eGFP
CK
PDX1
C
eGFP
Hoechst
SYP
Hoechst
INS
Hoechst
Merge
D
ECadCFP
mCppt
INS
Merge/Hoechst
E
ECadCFP
mCppt
INS
Merge/Hoechst
F
N. of cells
100
90
80
70
60
50
10
0
eGFP+
SYP+
INS+
CK+
Others

Figure 7

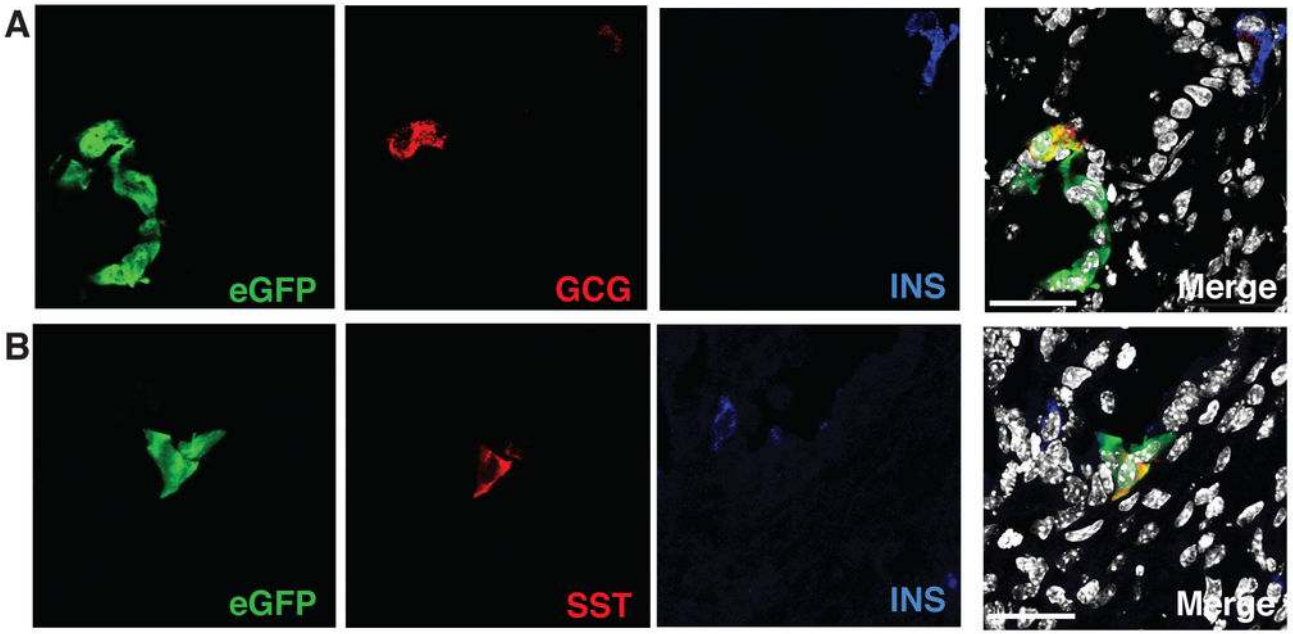

PDL-WT

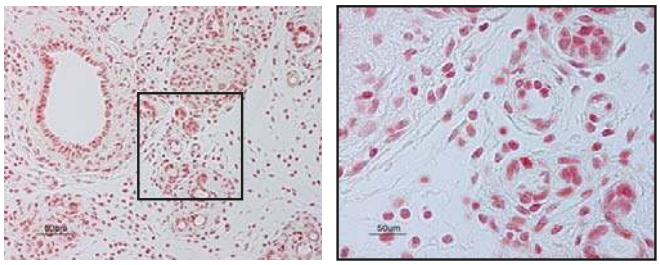

Supplementary FIGURE 1

A

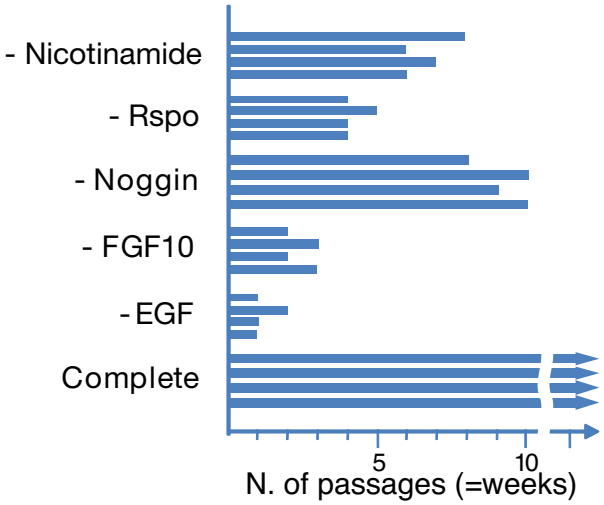

B

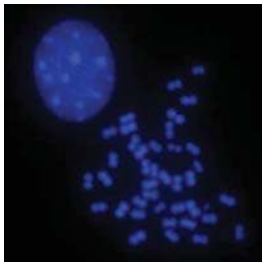

Chromosomal count
n=40

	2-3 weeks	2.5 months	5 months
n<39	11.11%	10.00%	0.00%
n=39	11.11%	10.00%	25.00%
n=40	55.56%	70.00%	75.00%
n>40	22.22%	10.00%	0.00%

C

2 weeks after transplantation

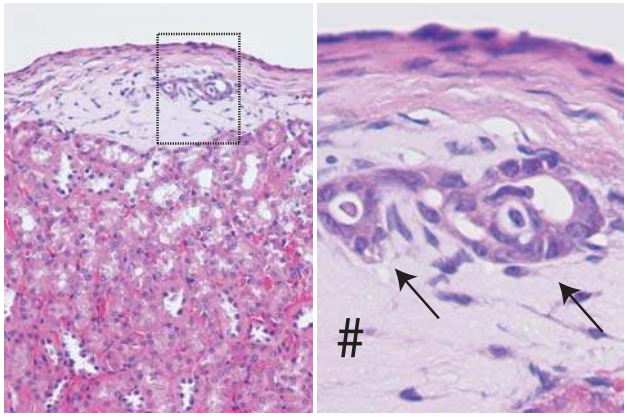

D

2 months after transplantation

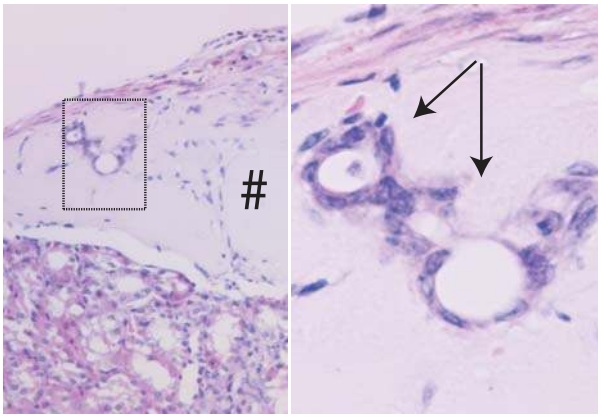

Supplementary Figure 2

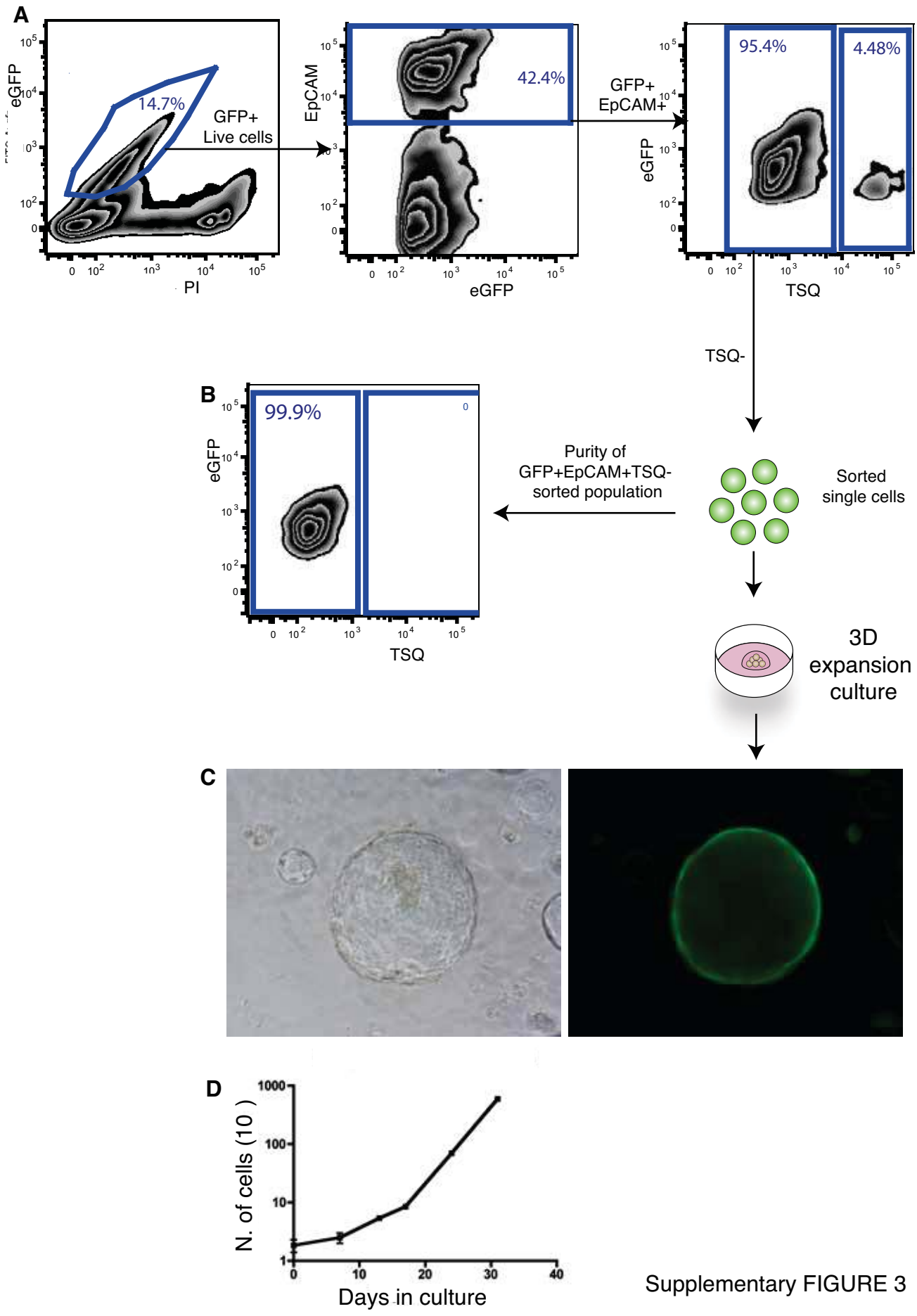
A
eGFP
14.7%
GFP+
Live cells
PI
EpCAM
42.4%
eGFP
GFP+
EpCAM+
eGFP
95.4%
4.48%
TSQ
TSQ-
B
99.9%
eGFP
TSQ
Purity of
GFP+EpCAM+TSQ-
sorted population
Sorted
single cells
3D
expansion
culture
C
D
N. of cells (10)
Days in culture
Supplementary FIGURE 3

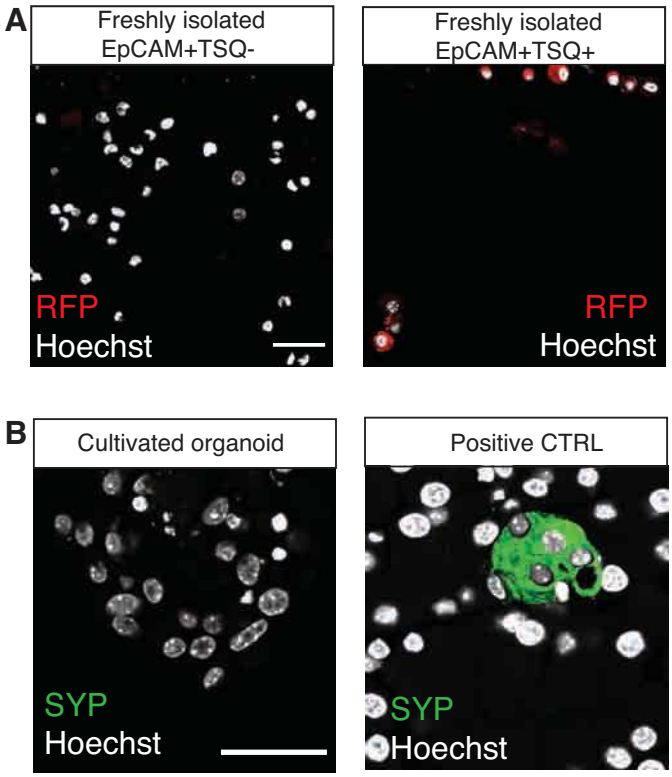

Supplementary FIGURE 4

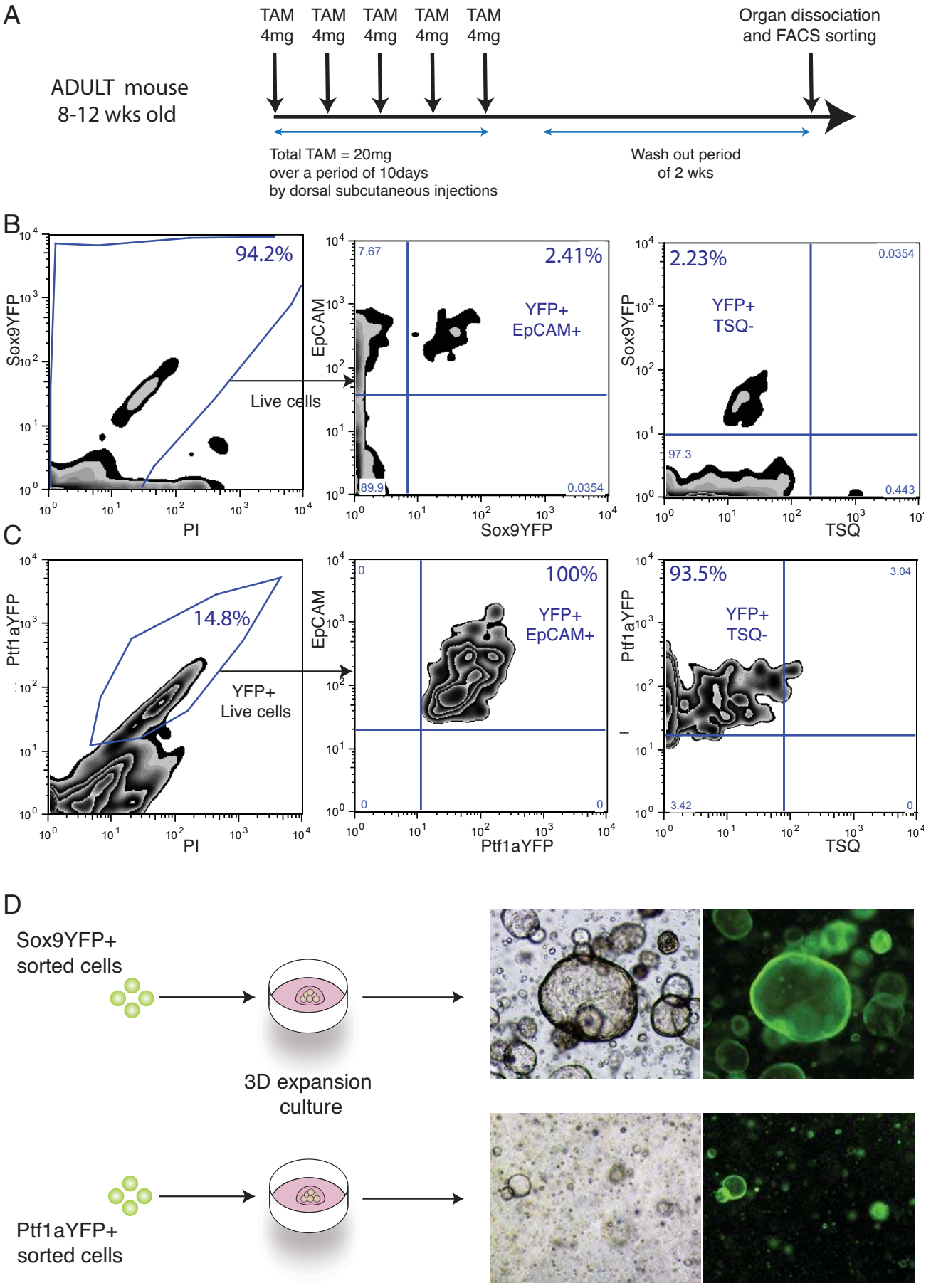

Supplementary FIGURE 5

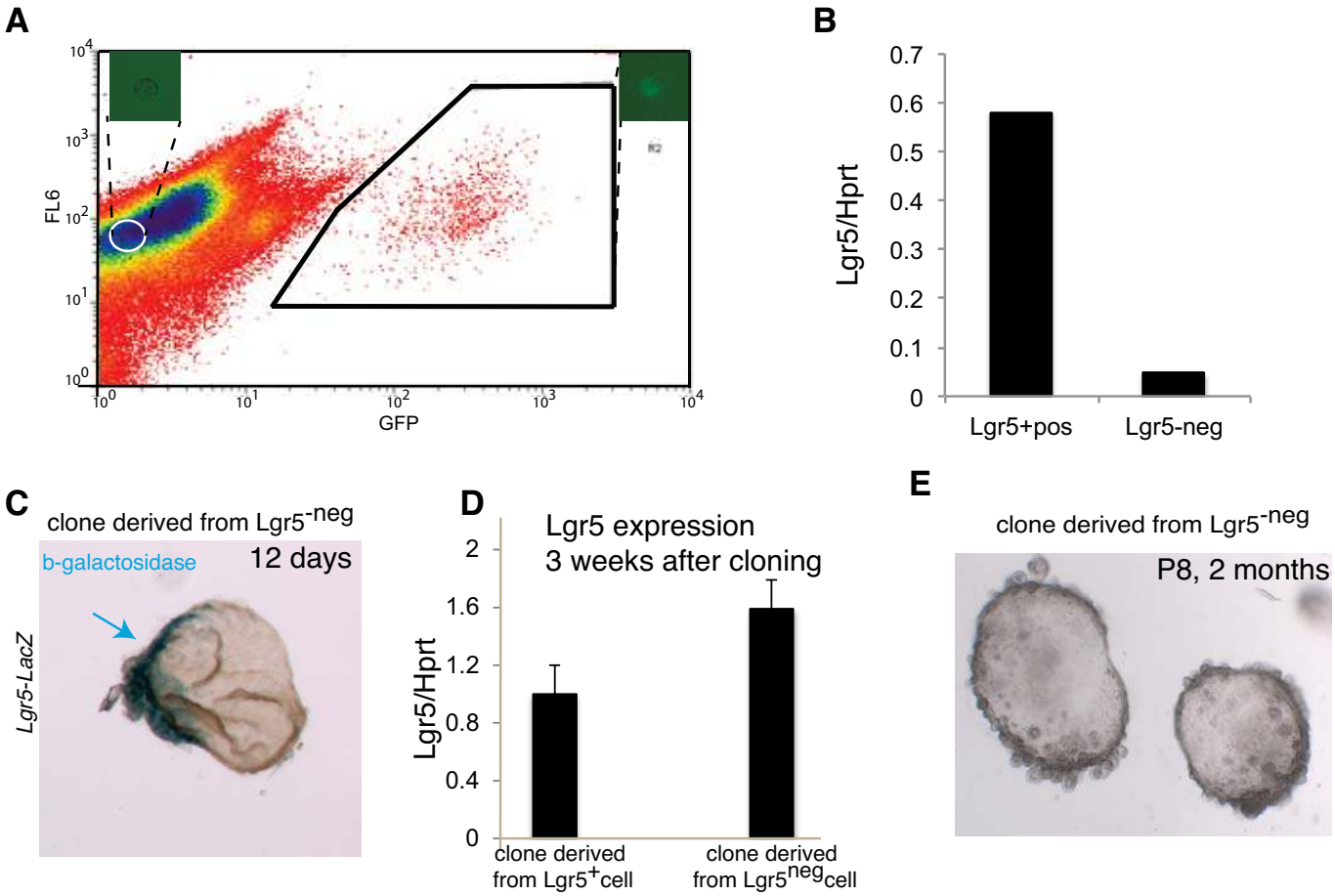

Supplementary Figure 6

Supplemetary Figure 7

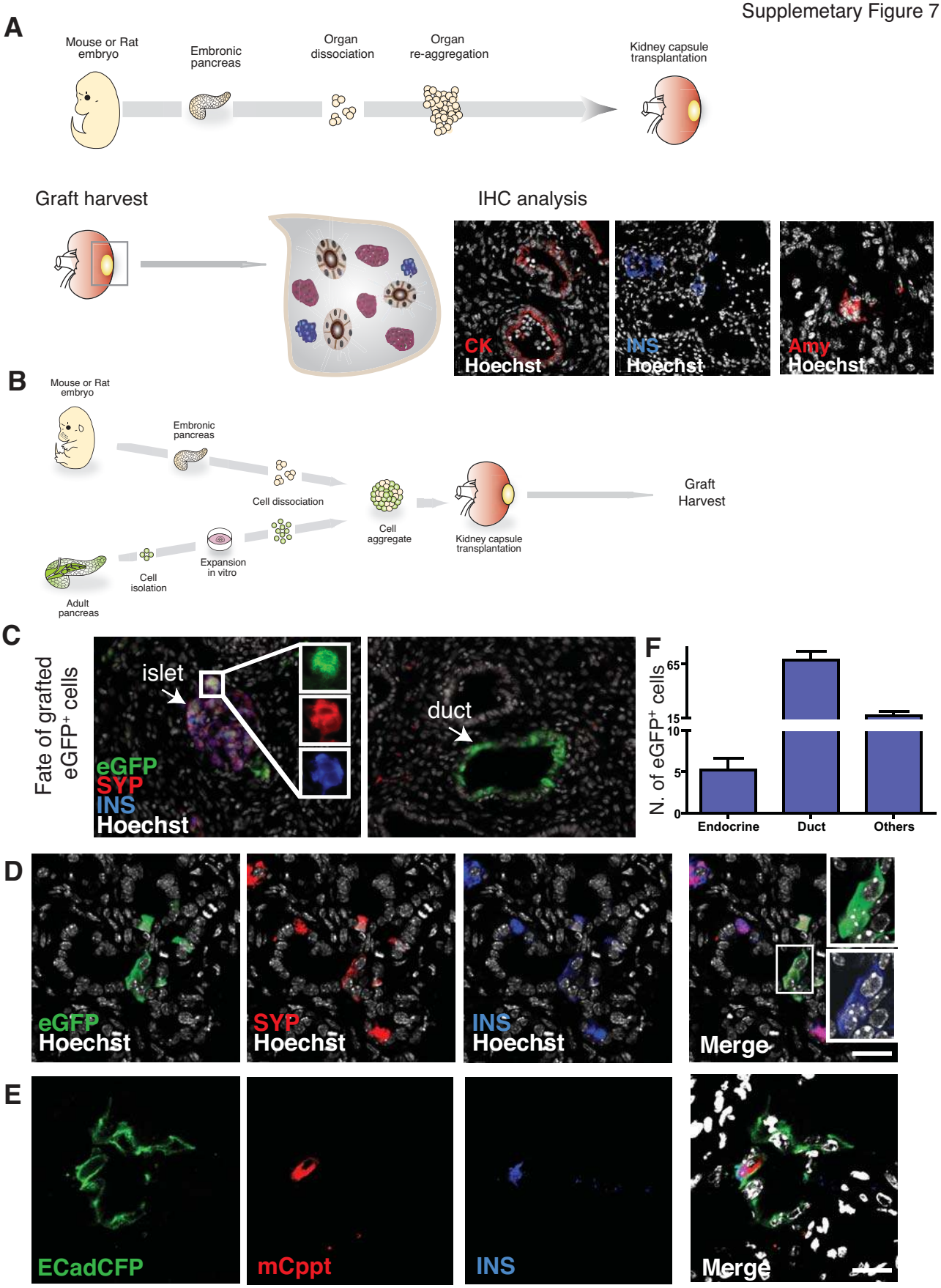

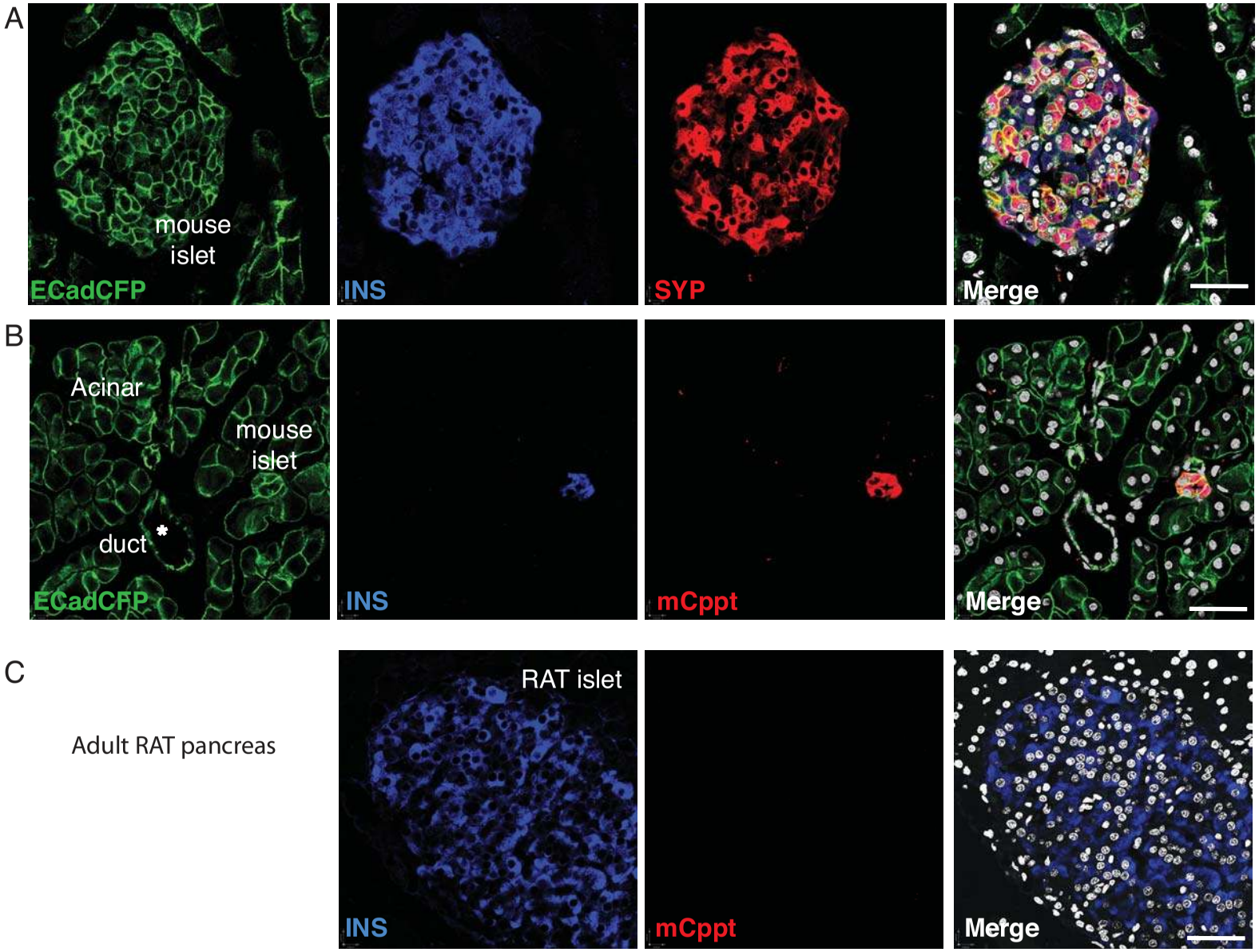

Supplementary Figure 8

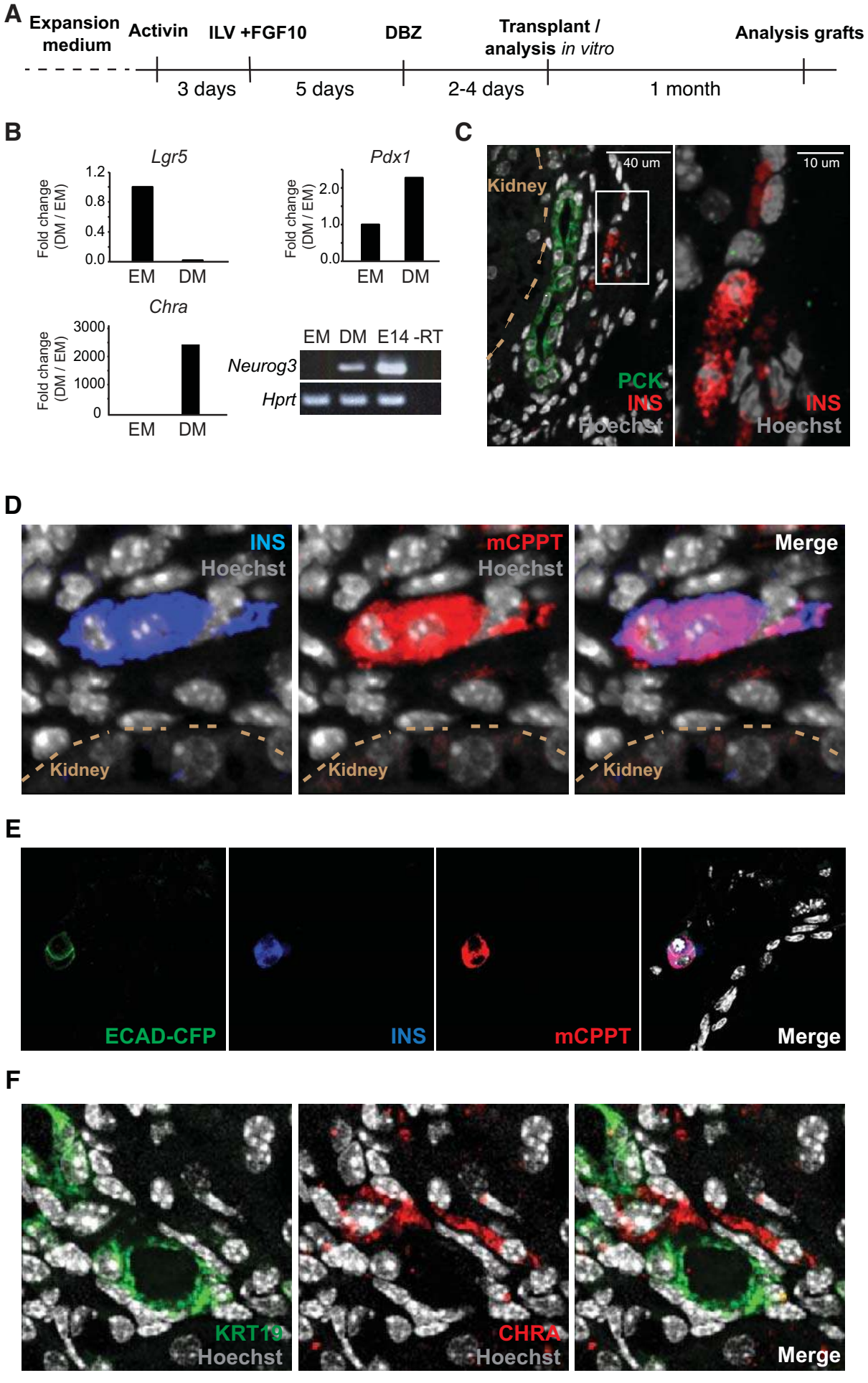

Supplementary Figure 9